

Plastination of pathological specimens – a new challenge

A Alpár^{1*}, T Glasz², Zs Fejér³, M Kálmán¹

¹Department of Anatomy, Histology and Embryology, Semmelweis University, Faculty of Medicine, Budapest, Hungary,

²Second Department of Pathology, Semmelweis University of Medicine, Budapest, Hungary, ³Department of Human Morphology and Developmental Biology, Faculty of Medicine, Semmelweis University, Budapest, Hungary

Numerous recent studies have acknowledged the merits of plastination in anatomy. Specimens conserved in this way can be handled easily and hygienically which broadens the possibilities in the presentation of anatomical preparates. The present study aimed to introduce plastination in another morphological discipline, in pathology. Conserving pathological organs or tissues with polymer impregnation and curing offered completely new challenges which have not been faced when plastinating healthy tissues. Transformed tissues often change their color or consistence, they can be removed or washed out easily in other cases, however, the preservation of these alteration is of primary diagnostical importance. It could be demonstrated that color differences could be preserved in many cases, fixation of loosely anchored tissues was possible. Subtle, but typical alterations on the surface of ill organs were demonstrable as well. At the same time, consistence differences between neighbouring healthy and pathological tissues completely disappeared which ment a loss in diagnostic cues. Regarding the large number and diverse kinds of plastinated specimens we can propose that plastination serves as a useful tool in preserving pathological tissues.

*Corresponding author

E-mail: alpar@ana.sote.hu

Evaluation of the potential therapeutic use of immature stem cells in a canine model for Duchenne muscular dystrophy

CE Ambrosio^{2*}, I Kerkis¹, DS Martins², A Kerkis³, M Vanizof⁴, SAS Fonseca¹, C Maranduba¹, RM Cabral², TG Peixoto², AC Morini², MP Brolio², LR Bertolini², MA Miglino², M Zatz⁴

¹Laboratório de Genética, Instituto Butantan, São Paulo, SP, Brasil, ²Departamento de Cirurgia da Faculdade de Medicina Veterinária da Universidade de São Paulo, SP, Brasil, ³Genética Aplicada, Atividades Veterinárias LTD, São Paulo, SP, Brasil,

⁴Centro de Estudos do Genoma Humano, Departamento de Genética e Biologia Evolutiva, Universidade de São Paulo, SP, Brasil

Duchenne muscular dystrophy (DMD) is a most severe form of muscular dystrophy, which is inherited as a sex-linked recessive trait and affects 1/3500 of newborn males. Molecular genetic studies indicate that MDM is the result of mutations in the huge gene that encodes dystrophin, and in 1/3 of the cases the disease is a result of a spontaneous or new mutation (Zatz 2000). In order to confirm the results obtained from mouse model, which did not provide clinical sings of the disease, it has been proposed that muscular dystrophy in the golden retriever dog may be homologous to human. Further investigation showed a normal karyotype, but a molecular defect in X-linked muscular dystrophy of the golden retriever dog (GRMD), thus demonstrating the authenticity of the canine model (Sharp et al. 1992; Valentine et al. 1992).

To compare two types of adult stem cells, umbilical cord CD 34⁺ and dental pulp stem cells (IDPSC), as potential multipotent stem cells for cell therapy use, by the evaluation of their skeletal myogenic potential, migration ability and capacity to restore dystrophin function in skeletal muscle cells of dystrophic young dogs.

Each cell type was analyzed according to their morphology, ultrastructure (confocal and TE microscopy), and cell culture ability. *In vivo* tests were carried out to analyze engraftment features after infusion of Dil-labeled cells, without any immune suppression, either into the femoral artery or by intramuscular injection of 30-days-old dystrophic dogs. After 60 days, biopsies were taken for tissue immunostaining with anti-IDPSC antibody developed in our laboratory. Clinical trials were made performing critical analyses of disease evolution. Results: By electronmicrography, canine umbilical cord stem cells had an immature cell structure, differing from all primitive blood components. Cell cultures showed poor proliferation for both cell types; consequently, fresh umbilical cord stem cells. Cells, obtained by density solution and magnetic separation, were used for injections into the biceps femoralis or the femoral artery. After 60 days, tissue biopsies failed to demonstrate the presence

of dystrophin either by immunohistochemistry or by protein blotting. Conversely, the analysis of tissue biopsies of animals injected with IDPSC showed denser cell engraftment, as indicated by both the presence of DiI-stained cells and anti-IDPSC antibody positive labeling. Clinical aspects were considered relevant, with the demonstration of significant differences depending on the route of injection and cell type.

The efficacy of arterial injection of pulp dental cells to treat muscular dystrophy demonstrated that canine multipotent stem cells have great potential for cell therapy, promising to become a new trend for therapeutical approaches aiming muscular dystrophy.

Sharp NJH, Kornegay JN, Van Camp SD, Herbreith MH, Secore SL, Kettle S, Hung W-Y, Constantinou CD, Dykstra MJ, Roses AD, Bartlett RJ (1992) An error in dystrophin mRNA processing in golden retriever muscular dystrophy, an animal homologue of Duchenne muscular dystrophy. *Genomics* 13:115-121.

Valentine BA, Winand NJ, Pradhan D, Moise NS, de Lahunta A, Kornegay JN, Cooper BJ (1992) Canine X-linked muscular dystrophy as an animal model of Duchenne muscular dystrophy: a review. *Am J Med Genet* 42:352-356.

Zatz M, Vainzof M, Passos-Bueno MR (2000) Limb-girdle muscular dystrophy: One gene with different phenotypes, one phenotype with different genes. *Curr Opin Neurology* 13:511-517.

*Corresponding author
E-mail: ceambrosio@usp.br

Improving the pregnancy rate in IVF with pre IVF fluid instillation sonohysterography (PIFIS) and ultrasound guided embryo transfer (UGET)

OA Ashiru*, AA Adewusi, LJ Shittu, M Oladimeji, R Ojugbo

IVF Unit, Medical Art Center, Mobolaji Bank Anthony Way, Ikeja, Lagos, Nigeria

Objective: A practical effort to improve pregnancy rate in in-vitro fertilization and embryo transfer by the instillation of a fluid cocktail of saline and antibiotics to artificial distend the uterine cavity in the cycle prior to IVF, and the use of ultrasound guided embryo transfer.

Design: Prospective study.

Setting: Private fertility clinic and Academic center.

Patient(s): 5 patients undergoing IVF and ICSI (Intracytoplasmic sperm injection) treatment with prior failed IVF cycle with hydrosalpinx or submucous fibroid and had to go through sonohysterography to exclude uterine abnormalities or evaluation and location of submucous fibroid in the cycle prior to the IVF cycle.

Intervention(s): A saline fluid containing antibiotics cocktails was instilled in the uterine cavity through a plastic intrauterine insemination catheter attached to a syringe. Transvaginal (3-dimensionnal) ultrasonography was performed concomitantly. After IVF and ICSI embryos were transferred with ultrasound guidance ensuring placement in upper uterine cavity.

Main Outcome Measure: Clinical pregnancy.

Result(s): One patient with severe hydrosalpinx distending into the uterine cavity got pregnant and delivered a baby boy, after prior failed attempt, another patient with submucous fibroid and prior failed IVF attempt is currently pregnant. Remaining three patients had ET done and are clinically pregnant.

Conclusion: The use of PIFIS and UGET does appear to improve the pregnancy outcome in IVF.

Support: supported by grants from OARS Foundation.

*Corresponding author
E-mail: denrele@tigger.uic.edu

The feline “peripulvinar” nucleus

ZsB Baldauf

Department of Anatomy, Szent-Györgyi Albert Medical School, University of Szeged, Szeged Hungary

The mammalian thalamus is embraced rostrally and laterally by a thin sheath of neurons, the thalamic reticular nucleus (TRN). The TRN is perfectly suited to monitor the entire thalamo-cortico-thalamic information exchange through the axon collaterals given off by the crossing ascending and descending fibers. In addition, the TRN can modulate the function of the thalamus through its powerful inhibitory projections to thalamic cells.

In the cat's TRN, an internal and an external tier can be discerned. It has been recently discovered that both tiers form modality specific sectors (e.g. visual, somatosensory etc.) and innervate selectively their thalamic counterparts. Furthermore, a well-established functional difference is known between the two layers of the TRN around the dorsal lateral geniculate nucleus (dLGN). The response of TRN cells in the outer tier depends more on cortical innervation, than on thalamic one, whereas the inner tier (or perigeniculate nucleus; PGN) responds better to optic nerve stimulation. It would be quite interesting to learn whether other sectors of TRN belonging to other thalamic nuclei show similar duality. In order to examine this problem, the visual sector of the feline TRN has been stained with various chemoanatomical markers and then the pulvinar (PUL) has been injected with neuroanatomical tracers.

Histochemical reactions against an intracellular cytoskeletal protein (SMI-32) and an extracellular matrix component (Wisteria floribunda agglutinin, WFA) were used to detect the layers of the TRN around the PUL. Whereas the WFA-binding labeled the perineuronal net around reticular perikarya and major dendrites, the SMI-32-immunoreaction stained quite intensely the perikarya and their dendrites till the distal portion providing a state-of-the-art morphological stain. Both markers, however, could visualize the typical fusiform reticular neurons. Curiously, the WFA-labeled neurons in the outer tier were larger than those in the inner tier, moreover the outer tier proved to be thicker than a rather slim inner one attaching really closely to the thalamus. These findings resulted in an apparent stronger WFA-staining in the outer layer around both the PUL and the dLGN. The SMI-32-immunoreaction detected this size difference of reticular neurons, as well.

Following a retrograde tracer injection into the PUL, two streaks of neurons were labeled in the TRN exclusively aside the PUL revealing a previously unknown reticular sector. Similarly to the dLGN, it seems that two TRN tiers exist laterally from the PUL specifically dealing with this thalamic nucleus. The location, chemoanatomy, and connections of this bilaminar TRN sector around the PUL resembled closely to the dLGN's one. Therefore, we propose to distinguish the outer tier around the PUL as TRN ‘proper’ and the inner tier as “peripulvinar” nucleus.

Supported by the “Fight for Sight”, NY (#03055) grant to ZBB.

E-mail: zsolt.baldauf@yahoo.com

Developmental redistribution of phototransduction proteins and modulating molecules in the hamster retina

Á Berta*, Á Lukáts, A Szabó, G Halász, A Magyar, P Röhlich, AL Kiss, Á Szél

Laboratory of Cell and Molecular Biology, Department of Human Morphology and Developmental Biology, Semmelweis University, Budapest, Hungary

The Sirian hamster (*Mesocricetus auratus*) is born blind. The newborn hamster retina is immature and exhibits a special structure. Following continuous maturation of the retina its structure becomes similar to that of the adult by day 14, when the eyes open. Our study aims at the distribution changes of the phototransduction cascade participants and modulators during the retinal development. During the lifetime of the rod cell, the supplement of rhodopsin is achieved by a continuous vesicular transport, from the cell body to the connecting cilium. The synthesis takes place in the cell body and the proteins are transported to the site of phototransduction, the outer segment. Caveolin-1 is a well-known organiser protein of polarised transport, which may suggest a role for detergent-resistant lipid rafts in the recruitment and formation of signaling complexes within photoreceptor outer segments. Our observations show that the distribution of these molecules changes in parallel

with the eye opening and the initiation of vision. We present additional evidence, that the localisation of caveolin-1, src, rhodopsin-kinase and rhodopsin show a similar pattern. The arrangement is similar not only at the location of the synthesis, but also during the intracellular transport. Double-label immunocytochemistry and immunoprecipitation were used to prove the colocalization of these molecules. Since caveolin-1 and src, typical components of lipid rafts, are also associated with this complex, presumably these molecules are connected by lipid rafts and their transport to the outer segments is modulated by caveolin-1. This latter protein may also have a role in the regulation of phototransduction.

*Corresponding author
E-mail: agnesberta@hotmail.com

Anatomical features of the aberrant extensors to the index finger and its clinical importance

O Bilge, F Govsa, Y Pinar*, S Celik

Department of Anatomy, Faculty of Medicine, Ege University, Izmir, Turkey

Independent ability to extend the index is necessary to know the existence of some variant muscles including, extensor indicis proprius (EI), extensor medii proprium (EMP) and extensor indicis medii proprium (EIMP) to the index finger. The EI, EMP and EIMP transferred for conditions such as lost function as a result of trauma, rheumatoid arthritis, ulnar nerve palsy, cervical spinal cord injury, and hypoplasia of the thenar muscle.

Fifty-four dissected hands were examined to study of the aberrant extensor tendons to the index finger. The aberrant tendons were classified the arrangements into six types from A to F.

In all 54 hands, a tendon originated from EI muscle belly and was inserted into ulnar side of the extensor digitorum (EDC) tendon for the index finger at the level of the metacarpal head. In 36 specimens (66.7%), only this tendon was found, and thus this type regarded Type A. In Type B, both of the bifurcated slips were situated on the ulnar side of the EDC tendon of the index finger in one case (1.85%). In four specimens (7.4%), the aberrant second tendon attached to the radial side of the dorsum of the index finger in Type C. In Type D, the radial tendon in the other case bifurcated at the middle level of the metacarpus specimens in two (3.7%) specimens. One of these slips was inserted into the radial side of the dorsum of the index finger. The other attached to the tendon of the extensor pollicis longus. In Type E, the Type D was added the EMP in two specimens (3.7%). In Type E, the supernumerary tendon as EMP was Type A in nine specimens (16.6%). In 12 hands (22.2%), the tendons of EMP was found. The EIMP was detected in a specimen (1.85%).

The existence of the supernumerary tendons of the index fingers is more frequently encountered on the ulnar side of the extensor digitorum-index than on the radial side. Knowledge of variant muscles and tendon multiplicity has clinical importance in cases of traumatized hand requiring tendonoplasty or tendon transfer operations.

- Browne EZ Jr, Teague MA, Snyder CC (1979) Prevention of extensor lag after indicis proprius tendon transfer. *J Hand Surg [Am]* 4(2):168-172.
- El-Badawi MGY, Butt MM, Al-Zuhair AGH, Fadel RA (1995) Extensor tendons of the fingers: Arrangement and Variations-II. *Clin Anat* 8:391-398.
- Gonzalez MH, Weinzwieg N, Kay T, Grindel S (1996) Anatomy of the extensor tendons to the index finger. *J Hand Surg [Am]* 21(6):988-991
- Hirai Y, Yoshida K, Yamanaka K, Inoue A, Yamaki K, Yoshizuka M (2001) An anatomic study of the extensor tendons of the human hand. *J Hand Surg [Am]* 26(6):1009-1015
- Kitano K, Tada K, Shibata T, Yoshida T (1996) Independent index extension after indicis proprius transfer: excision of juncturae tendinum. *J Hand Surg [Am]* 21(6):992-996
- Komiyama M, Nwe TM, Toyota N, Shimada Y (1999) Variations of the extensor indicis muscle and tendon. *J Hand Surg [Br]* 24(5):575-578.
- Low CK, Pereira BP, Chao VT (2001) Optimum tensioning position for extensor indicis to extensor pollicis longus transfer. *Clin Orthop Relat Res* (388):225-232.
- Rockwell WB, Butler PN, Byrne B (2000) Extensor tendon: Anatomy, injury, and reconstruction. *Plast Reconstr Surg* 106:1592-1603.
- Von Schroeder HP, Botte MJ (1991) The extensor medii proprius and anomalous extensor tendons to the long finger. *J Hand Surg [Am]* 16(6):1141-1145.
- von Schroeder HP, Botte MJ (1995) Anatomy of the extensor tendons of the fingers: variations and multiplicity. *J Hand Surg [Am]* 20(1):27-34.
- von Schroeder HP, Botte MJ (1993) The functional significance of the long extensors and juncturae tendinum in finger extension. *J Hand Surg [Am]* 18(4):641-647.

*Corresponding author
E-mail: yeldapinar@gmail.com

Effect of pulsed radiofrequency on nitroxidergic system in a model of neuropathic pain in rat

E Borsani^{1*}, S Sangiorgi², M Protasoni³, R Albertini¹, C Dell'Orbo², G Tomei³, R Bianchi¹, LF Rodella¹

¹Unit of Human Anatomy, Department of Biomedical Sciences and Biotechnologies, University of Brescia, Brescia, Italy,

²Department of Surgery, Neurosurgical Unit, University of Insubria, Varese, Italy, ³Department of Human Morphology, University of Insubria, Varese, Italy

Pulsed radiofrequency (PRF) has been ascribed among the most promising non-invasive methods for the treatment of neuropathic pain (Sluijter 1998), nevertheless its mechanism of action has not been still clarified. Nitric oxide is involved in pain modulation both at peripheral and central nervous system (Rodella 1998; Cizkova 2002).

The aim of this work was to monitor the effect of PRF on nitroxidergic system in DRGs, spinal cord and PAG (periaqueductal grey matter) in a neuropathic pain model.

Experiment was carried out on 18 male Sprague-Dawley rats.

The animals were subdivided into two groups: 1) non-operated animals; 2) operated animals, in which the left sciatic nerve was tied (chronic constriction injury - CCI) according to Bennett and Xie (1998). The half of the animal of each group was treated with PRF, whereas the others were used as an untreated control. PRF was performed at 7th post-operative day and monitored at 14th post-operative days. The animals were killed and the DRGs, lumbar spinal cord (L4-L6) and midbrain were removed, frozen and then processed for nNOS immunohistochemistry.

In operated (CCI) animals we observed a significant increase in nNOS immunostaining intensity in the small neurons of DRGs; an increase of nNOS- positive neurons at spinal cord level and a decrease of nNOS-immunostaining in dorsolateral area of the PAG. In the animals treated with PRF, the pattern of nNOS was similar to the control group.

Our data showed that PRF modulates nNOS both in peripheral and central nervous system suggesting a direct effect of PRF on nitroxidergic system.

Bennett GJ, Xie YK (1998) A peripheral mononeuropathy in rat that produces disorders of pain sensation like those seen in man. *Pain* 33:87-107.

Cizkova D, Lukacova N, Marsala M, Marsala J (2002) Neuropathic pain is associated with alterations of nitric oxide synthase immunoreactivity and catalytic activity in dorsal root ganglia and spinal dorsal horn. *Brain Res Bull* 58:161-71.

Rodella L, Rezzani R, Agostini C, Bianchi R (1998) Induction of NADPH-diaphorase activity in the rat periaqueductal gray matter after nociceptive visceral stimulation. *Brain Res* 793:333-6.

Sluijter M, Cosman E, Rittman W, van Kleef M (1998) The effects of pulsed radiofrequency fields applied to the dorsal root ganglion. A preliminary report. *Pain Clinic* 11:109-117.

*Corresponding author

E-mail: eborsani@med.unibs.it

Caveolae mediated endocytosis in HepG2 cells: caveosomes or lysosomal degradation

E Botos^{1*}, J Klumperman², V Oorshot², B Igyarto¹, A Magyar¹, M Oláh¹, AL Kiss¹

¹Department of Human Morphology and Developmental Biology, Semmelweis University, Budapest, Hungary,

²Cell Microscopy Center, Department of Cell Biology, University Medical Center, Utrecht, The Netherlands

Nowadays it is generally accepted that, under special conditions, caveolae can take part in ligand internalization. Endocytosis via caveolae is a slow, highly regulated process exists as alternative endocytic machinery parallel to clathrin-dependent endocytosis. Along the caveolar pathway, caveosomes were described as intermediate organelles, characterized only by the presence of caveolin-1 at their limiting membrane. Ligands endocytosed by clathrin-coated pits, however, were never detected in caveosomes. At present, there is no evidence indicating or excluding the potential communication between caveosomes and the organelles of the classical endocytic pathway.

In our work we were especially interested in what can be the further intracellular fate of caveolin-1 and caveosomes. To

answer this question we followed the route of caveolae/caveolin-1 in HepG2 cells by immunocytochemistry on ultrathin frozen sections and Western blot analysis of purified membrane fractions under the inductive effect of albumin.

We found that the number of caveolae at the plasma membrane strongly depended on the presence of albumin. As it was expected albumin induced the internalization of caveolae. To study whether caveolar endocytotic machinery can join to the classical endocytotic pathway, late endosomes/lysosomes and caveolae were labeled with anti-CD63 (LIMP-1), and anti-caveolin-1 antibodies on ultrathin frozen sections respectively. Long term (1 and 3 hours) albumin treatment resulted in the appearance of albumin containing caveolae in special multicaveolar complexes and caveosome-like structures. Numerous late endosomes/multivesicular bodies were characterized by CD63 (LIMP-1) contained caveolin-1 suggesting that caveolin-1 entered the degradative pathway. Our Western blot analysis showed that albumin uptake resulted in a significant decrease of caveolin-1 in the cytoplasmic membranes (including late endosomes and lysosomes) providing further evidence about the degradation of caveolin-1. Inhibition of the endosomal and lysosomal fusion by monensin has not changed the level of caveolin-1 present in the cytoplasmic membranes. Cycloheximide treatment blocked the appearance of caveolin-1 on the plasma membrane indicating that protein synthesis is necessary for new caveolae formation.

*Corresponding author
E-mail: berbet@ana2.sote.hu

The adaptability, flexibility and versatility of haematopoietic stem cells

D Brynmor-Thomas

Bute Medical School, St Andrews, Scotland, UK

Stem cell populations are not characterized by the possession of distinctive morphological features but can be defined operationally using their ability to maintain self-renewal while providing an appropriate output of precursors to one or more maturation compartments. They must therefore be capable of generating new stem cells and strictly speaking a transplanted stem cell population should be capable of restoring a depleted population in a primary recipient and subsequently in a secondary recipient. The immediate progeny of stem cells are termed "progenitor cells", which provide an appropriate output of precursors to one or more lineages. Progenitor cells lose the ability to maintain self-renewal but are distinguished by their enormous clonogenic capacity. The ability of a stem cell population to respond to variable demands thus depends upon the susceptibility of its progenitor cell output to regulatory mechanisms. This is correctly termed "stem cell plasticity", a term frequently used to designate the versatility of self-maintaining cell populations, although it does not differentiate between their versatility, flexibility and adaptability. The adaptability of a stem cell population can be defined as the ability to adjust its output of precursors to a single maturation compartment, which can for instance enable the rate of proerythroblast production to be increased in response to hypoxia. Adaptability can usefully be distinguished from flexibility, the ability of a multipotent stem cell population to regulate the distribution of such adjustments between two or more maturation compartments and versatility, the ability of a stem cell population to contribute to the production of previously unexpected progeny. The concept of stem cell versatility has been generated during the past decade or so by the demonstration of donor specific markers and the concurrent expression of cell specific markers in transplanted bone marrow-derived cells, which appear to have been assimilated into several populations of host cells derived from each of the three germ layers. The initial contention that versatility can be attributed to the trans-differentiation of transplanted cells has subsequently been endorsed. The use of host specific markers, in addition to donor specific markers and cell specific markers, has however revealed the formation of hepatocytes, skeletal muscle fibres and neurons in which heterokaria that have derived markers from both the donated cells and the cells of the host reflect the fusion of donor cells with host cells. It has thus become evident that while versatility may depend upon trans-differentiation, apparent versatility may result from cell fusion. These alternatives may both be important during development and regeneration as well as in cell replacement therapy. In some instances the replacement of damaged host cells by donor cells, with or without trans-differentiation, may be the only available option but in others the modification of viable but imperfect host cells by fusion with donor cells may be infinitely preferable. Thus following the destruction of irradiated blood cell precursors replacement is essential, whereas the modification of liver cells deficient in a single enzyme is a far more elegant alternative, if the polyploid heterokaria and the reprogrammed genes generated following fusion are not

potentially dangerous. In interpreting apparent versatility it remains important to recognize that in some instances it may be due to the heterogeneity of donor cell populations. While precise information is being accumulated about stem cell plasticity, attempts to develop stem cell replacement therapy will no doubt continue and include attempts to use bone marrow derived cells to replace or modify deficient or defective cells in the myocardium, the liver, the nervous system and elsewhere as well as in the bone marrow itself. These attempts can reasonably be encouraged - provided that their use is carefully monitored and rigorously evaluated.

(The generous support of the Margaret Rodger Research Fund is gratefully acknowledged.)

*Corresponding author
E-mail: dbt@st-and.ac.uk

Layer V/VI spiny inverted neurons

JL Bueno-Lopez*, JL Mendizabal-Zubiaga, JC Chiara, C Reblet

Department of Neurosciences, School of Medicine and Dentistry, The University of the Basque Country, Leioa (Vizcaya), Spain

In this paper, we present an account of past and current research being carried out on spiny inverted neurons — alternatively also known as “inverted pyramidal neurons” — in rats, rabbits and cats. In our laboratory, we have studied these cells with a battery of techniques suited for light and electron microscopy, including Nissl-staining, Golgi-impregnation, dye intracellular-filling and axon retrograde-track-tracing. Our results show that spiny inverted neurons make up less than 8.5% and 5.5% of all cortical neurons in the primary and secondary rabbit visual cortex, respectively. Infragranular spiny inverted neurons constitute 15% and 8.5% of infragranular neurons in the said animal and areas. Spiny inverted neurons congregate at layers V-VI in all studied species.

Studies have also revealed that spiny inverted neurons are excitatory neurons which furnish axons for all sorts of cortico-cortical, cortico-claustral and cortico-striatal projections, but not for non-telencephalic centres such as the lateral and medial geniculate nuclei, the colliculi or the pons. As a group, each subset of inverted cells contributing to a given projection is located below the pyramidal neurons whose axons furnish the same centre. Spiny inverted neurons are particularly conspicuous as a source of the backward cortico-cortical projection to primary visual cortex and from this to the claustrum. Indeed, they constitute up to 82% of the infragranular cells that furnish these projections.

Spiny inverted neurons may be classified into three subtypes according to the point of origin of the axon on the cell: the somatic basal pole which faces the cortical outer surface, the somatic flank and the reverse apical dendrite. As seen with electron microscopy, the axon initial segments of these subtypes are distinct from one another, not only in length and thickness, but also in the number of received synaptic boutons.

All of these anatomical features together may support a synaptic-input integration which is peculiar to spiny inverted neurons. In this way, two differently qualified streams of axonal output may coexist in a projection which arises from a particular infragranular point within a given cortical area; one stream would be furnished by the typical pyramidal neurons, whereas spiny inverted neurons would constitute the other source of distinct information flow.

Work granted by MEC-BSA2001-1179 & 9/UPV00212.327-15837/2004.

*Corresponding author
E-mail: joseluis.bueno@ehu.es

Aspects of the vascular disposal in the human rectal wall

R Cergan*, MA Banu, MC Rusu, RC Ciuluvica

Department of Anatomy, Carol Davila University of Medicine and Pharmacy, Bucharest, Romania

We used specimens from human foetus (7 and 8 months aged) that have been injected with China ink and formalin 10%. We observed the following vascular features: a) the rectal submucosa presents two arterial plexuses—one at the junction with the muscular coat, that supplies the submucosa and the circular muscular fibres, the other at the junction with muscularis mucosa, which supplies the epithelium and the mucous glands; b) in the middle part of the submucosa there are large, longitudinal veins; c) in the muscular coat there are elongated capillaries, parallel disposed with the muscular fibres; d) at the level of the anal columns there are granular arterio-venous anastomoses, the rectal glomeruli.

*Corresponding author
E-mail: anatonon@gmail.com

Vascular peculiarities in the human urinary bladder and vesicourethral junction

R Cergan*, MA Banu, MC Rusu, RC Ciuluvica

Department of Anatomy, Carol Davila University of Medicine and Pharmacy, Bucharest, Romania

We made our study on three human fetuses aged 29, 30 respectively 32 weeks, the vascular and muscular differentiations being in the final stage, in this period of the intrauterine development; the specimens have been injected with China ink and formalin 10%. Our attention was focused on the arrangement of the blood vessel in the wall of the urinary bladder and of the vesicourethral junction and we found two types of arterial disposal in the detrusor, due probably to the particular arrangement of the muscular fibers: a parietal type, in the wall of the urinary bladder and a junctional type, at the level of the vesicourethral junction.

*Corresponding author
E-mail: anatonon@gmail.com

Bilateral asymmetry in Subjects with cleft lip and palate

A Didilescu^{1*}, V Nimigean¹, N Maru¹, V Nimigean², S Stratul³, N Galie¹

¹Department of Anatomy and Embryology, Faculty of Dental Medicine, Carol Davila University of Medicine and Pharmacy, Bucharest, Romania, ²Department of Oral Rehabilitation, Faculty of Dental Medicine, Carol Davila University of Medicine and Pharmacy, Bucharest, Romania, ³Department of Periodontology, Faculty of Dental Medicine, Victor Babes University of Medicine and Pharmacy, Timisoara, Romania

Clefting of the lip and palate is one of the most frequent human major birth defects. All degrees of clefting may occur, ranging from the nondysfunctional submucous cleft to the major incapacitating forms of combined cheilouranoschisis. Facial clefts in humans are often associated with delayed development of dentition on the affected side comparing to the noncleft side as well as anomalies of number, size and shape of teeth on both sides (Larson et al. 1998; Harris 2002; Aizenbud et al. 2005). The aim of the present work is to provide a review of fluctuating and directional asymmetry in patients with cleft lip and palate, including features of tooth development. Several studies have demonstrated that lip-palate clefts are twice as common on the left side as the right (Sayetta et al. 1989; Vanderas and Ranalli 1989). The asymmetry that occurs in subjects with cleft lip palate can be explained by a hypothesis of Van Valen (1962). Bilateral asymmetry was classified into three kinds: (1) directional asymmetry, (2) antisymmetry, and (3) fluctuating asymmetry. Directional asymmetry occurs when a structure on one

side of the body is systematically larger than its antimere, or an unpaired structure characteristically is located to one side of the midline. Facial clefts are an example of directional asymmetry (Harris 2002). The pattern of cell movements is directed by the pattern of gene expression, which determines cell surface properties and motility. The left-right anatomical asymmetry of the vertebrate body is foreshadowed by left-right asymmetry in the pattern of gene expression in the early embryo (Alberts et al. 2002). On the other hand, a left-right asymmetry in mesiodistal dimensions in subjects with unilateral clefts suggests a fluctuating asymmetry. The concept is that the same genetic and environmental factors control growth of the left and right structures of the body; reduced homeostasis causes differences in size and shape of the bilateral structures (Harris 2002). Fluctuating asymmetry affects permanent teeth in patients with cleft lip and palate. Microdontia, hypodontia, hyperodontia, atypical tooth buds are the symptoms most frequently recorded (Stahl et al. 2006). Asymmetry is more advanced in the cleft area, reflecting low regulatory control during development.

- Aizenbud D, Camasuvi S, Peled M, Brin I (2005) Congenitally missing teeth in the Israeli cleft population. *Cleft Palate Craniofac J* 42:314-317.
- Alberts B, Johnson A, Lewis J, Raff M, Roberts K, Walter P (2002) *Molecular biology of the cell*. New York: Garland Science, pp. 1220-1222.
- Harris EF (2002) Dental development and anomalies in craniosynostoses and facial clefting. In Mooney MP, Siegel MI, eds. *Understanding craniofacial anomalies. The ethiopathogenesis of craniosynostoses and facial clefting*. New York: Wiley-Liss, Inc. pp. 425-467.
- Larson M, Hellquist R, Jakobsson OP (1998) Dental abnormalities and ectopic eruption in patients with isolated cleft palate. *Scand J Plast Reconstr Surg Hand Surg* 32:203-212.
- Sayetta RB, Weinrich MC, Coston GN (1989) Incidence and prevalence of cleft lip and palate: what we think we know. *Cleft Palate J* 26:242-248.
- Stahl F, Grabowski R, Wigger K (2006) Epidemiology of Hoffmeister's "genetically determined predisposition to disturbed development of the dentition" in patients with cleft lip and palate. *Cleft Palate Craniofac J* 43:457-465.
- Van Valen L (1962) A study of fluctuating asymmetry. *Evolution* 16:125-142.
- Vanderas AP, Ranalli DN (1989) Evaluation of craniomandibular dysfunction in children 6 to 10 years of age with unilateral cleft lip and palate: a clinical diagnostic adjunct. *Cleft Palate J* 26:332-337.

*Corresponding author
E-mail: andreea.didilescu@gmail.com

Normal and pathological aspects of the temporomandibular joint

A Didilescu^{1*}, M Enache², R Burcin¹, L Podoleanu¹, R Ivascu¹, N Galie¹, E Podoleanu³

¹Department of Anatomy and Embryology, Faculty of Dental Medicine, Carol Davila University of Medicine and Pharmacy, Bucharest, Romania, ²Department of Orthodontics and Dento-Facial Orthopedics, Faculty of Dental Medicine, Carol Davila University of Medicine and Pharmacy, Bucharest, Romania, ³Department of Medical Informatics and Biostatistics, Faculty of Dental Medicine, Carol Davila University of Medicine and Pharmacy, Bucharest, Romania

The temporomandibular joint (TMJ) is a synovial sliding-ginglymoid joint. It consists of the mandibular fossa and the articular tubercle (on the undersurface of the squamous part of the temporal bone), and the condyle (supported by the condylar process of the mandible). A fibrous disk divides the joint cavity into the superior and inferior compartments and is a structure with an important functional role: it provides a passive movable articular surface accommodating the translatory movement made by the mandibular condyle. The pathology of TMJ includes disk dislocations, quite frequent in young ages. There are many pathological situations in the TMJ functionality, one of them being the disk displacement with or without repositioning. All the conditions that allow the articular ligaments elongation and disk narrowing are involved in its etiology. One of the most common causes for that is the trauma, with two possibilities – micro and macro trauma. The elongation of the articular ligaments reduces the disk capacity of turning back simultaneously with the condyle, during mouth closing, so that at the end of the movement, the disk will be positioned more anterior, and the condyle will be in contact with the posterior part of the disk. As time will go by, the later will get thinner, the anterior position being accentuated and at the end of the mouth closing movement the condyle will lose its relationship with the disk, so that the mouth opening movement will be blocked. The authors present a case of a female patient diagnosed with a class II div 2 malocclusion, who came to the Department of Orthodontics and Dento-Facial Orthopedics because of a reduction of the mouth opening movements. The patient was diagnosed with a disk dislocation without reduction. She underwent a treatment that aimed first the relocation of the disk, followed by orthodontic treatment.

*Corresponding author
E-mail: andreea.didilescu@gmail.com

The effect of thyroid hormone substitution on M/L-cone development in *in vitro* organotypic retinal culture

V Doma, G Halász, A Szabó, Ál Berta, D Végyvári, P Röhlich, Á Szél, Á Lukáts*

Department of Human Morphology and Developmental Biology, Semmelweis University, Budapest, Hungary

The retina of most mammalian species contains two types of cones, one population being sensitive to shorter wavelengths (S-cones), and another one with the a peak sensitivity in the green or in the red part of the spectrum (M/L-cones). According to the widely accepted theory of transdifferentiation, these two populations do not develop independently from each other. All cones first express the S-opsin only, and some of them continue to do so till adulthood (genuine S-cones). The rest of the cones switch on M/L-opsin production as well, coexpress both pigments for a limited time interval (transitory photopigment coexpression), then S-opsin disappears from their inner segments. Despite intensive studies, little is known about the factors influencing this pigment switch. The putative candidates (e.g.: thyroid hormones, retinoic acid, growth factors and their receptors) are numerous, their precise role however is mostly unknown.

The most common animal models to study the possible regulatory factors are based on rat and mouse retinas. The disadvantage of all these approaches is that these species have at least two cone populations, thus each factor may independently influence the development of both cone types, and their interaction may also modify the results. In the mouse a dorso-ventral gradient could also be detected in the expression of opsin types, making the interpretation of the results even less reliable.

Hereby, we suggest a new model animal to study the possible regulatory factors of M/L-cone differentiation. The Syrian golden hamster as reported here possesses a retina that is devoid of genuine S-cones. The one single cone population expresses the M/L-pigment only, an ideal situation for developmental investigations. The retina also exhibits full differentiation even *in vitro* organotypic retinal cultures, under control conditions. Analyzing and comparing the retinal development of this species *in vivo* and *in vitro*, under different culturing conditions allow us to estimate the effect of regulatory factors in a homogeneous cone system. The first series of experiments reported here, focused on thyroid hormones that were known to play a decisive role in mouse M/L-cone development.

For *in vivo* retinal culturing retinas of Syrian golden hamsters (D0-4) were explanted onto a semiporous membrane and cultured till D14. The culturing media contained DMEM and HEPES (1:1) supplemented by hormones and vitamins, with or without serum (10% FCS) added. After fixation, the retinas were analyzed by immunocytochemistry.

Our results show that unlike in the mouse, thyroid hormone deprivation does not influence M/L-cone differentiation in the Syrian hamster. In all types of media, both supplemented with, or devoid of thyroid hormone M/L-cones were detectable in comparable quantity and exhibiting similar morphology. In serum free medium, on the other hand, practically no M/L-cones were present, and differentiation was not completed even when hormone was substituted in excess. These results demonstrate that some unknown factor - rather than thyroid hormone - is present in the serum that is necessary for cone differentiation in the Syrian golden hamster, indicating that cone development may be controlled by a different mechanism in this species.

The experiments have been supported by the following grants: Hungarian Scientific Research Fund (OTKA #T-042524, #F-61717).

*Corresponding author
E-mail: lukats@ana2.sote.hu

Myofibroblasts vs. smooth muscle cells - peritubular contractile cells in the testis of the dog

GF Egger, K Witter*

Histology and Embryology, Department of Pathobiology, University of Veterinary Medicine Vienna, Vienna, Austria

Contractile cells in peritubular tissue of the mammalian testis are supposed to contribute to the initial transport of spermatozoa from testis to epididymis. These cells are usually referred to as myoid cells without further classification. However, in some species such as cattle and humans, they have been termed myofibroblasts (Böck et al. 1972; Wrobel et al. 1979; Hees et al. 1989). The aim of this study was to assess the distribution of peritubular contractile cells in the canine testis by immunohistochemistry and transmission electron microscopy and to classify them with respect to their possible physiologic function. The complete tubular system of the canine testis, including seminiferous tubules, rete channels, efferent ducts and ductus epididymidis, is surrounded by contractile cells expressing smooth muscle actin, smooth muscle myosin and desmin. Contractile cells of seminiferous tubules and efferent ducts represent smooth muscle cell (SMC)/myofibroblast intermediates with different morphology, but both showing structural characteristics of SMC (e.g. spindle shape and nucleus with smooth surface) as well as of myofibroblasts (e.g. incomplete basement membrane). Contractile cells surrounding rete channels represent typical stellate myofibroblasts with incomplete basement membrane, stress fibres and lobated nucleus, those of the ductus epididymidis spindle-shaped SMC with complete basement membrane, spindle-shaped nucleus and uniformly distributed microfilaments. Differences in structure and arrangement of these peritubular contractile cells suggest different functions. Myofibroblasts and contractile cells similar to them, which surround seminiferous tubules, rete channels and efferent ducts, are probably mainly responsible for maintenance of an appropriate tissue turgor, whereas contraction of SMC of the ductus epididymidis might cause true peristaltic movement and therefore propulsion of spermatozoa. Experimental studies with isolated tubular segments would be helpful to prove this hypothesis.

Böck P, Breitenecker G, Lunglmayr G (1972) Kontraktile Fibroblasten (Myofibroblasten) in der Lamina propria der Hodenkanälchen vom Menschen. *Z Zellforsch* 133:519-527.

Hees H, Wrobel KH, Kohler T, Abou Elmagd A, Hees I (1989) The mediastinum of the bovine testis. *Cell Tiss Res* 255:29-39.

Wrobel KH, Mademann R, Sinowatz F (1979) The lamina propria of the bovine seminiferous tubule. *Cell Tissue Res* 202:357-377.

*Corresponding author

E-mail: kirsti.witter@vu-wien.ac.at

Ultrastructural analysis in human gingival fibroblasts after exposure to hema

M Falconi, G Teti, M Zago, M Ortolani, A Ruggeri Jr, L Breschi, G Mazzotti*

Department of SAU&FAL, University of Bologna, Bologna, Italy

Polymerized resin-based dental materials can release monomers from their matrix due to an incomplete polymerization or degradation processes. Released monomers can diffuse in the oral cavity and induce adverse effects to biological tissues. Although there are many data about the effects of lethal concentrations of resin monomers, a few studies have been conducted to investigate morphological modifications of cells exposed to sub lethal concentrations of dental monomers.

The aim of this study is to analyze ultrastructural modifications in human gingival fibroblasts exposed to a sub lethal concentration of HEMA and to analyze the influence of dental monomers on the expression of the protein procollagen $\alpha 1$ type I. A primary culture of gingival fibroblasts were exposed to 3 mM HEMA for 24 h, 72 h, 96 h. Morphological investigations were performed by scanning electron microscopy and transmission electron microscopy, while an immunostaining for fluorescence microscopy was carried out to visualize the protein procollagen $\alpha 1$ type I.

A strong modification in cell morphology from a fibroblastic shape to a round shape due to HEMA treatment was demonstrated by scanning electron microscopy. These results correlate with the transmission electron microscopy data which showed

deep changes in the cytoplasm after 72 h and 96 h. Immunofluorescence demonstrated a high signal of procollagen $\alpha 1$ type I around nucleus. This localization and the intensity of the signal decreased with the treatment and are in agreement with our molecular biology data which demonstrated a decrease of procollagen $\alpha 1$ type I both in its synthesis and expression.

These findings suggest that the sub-lethal concentration of HEMA tested has toxic effects on gingival fibroblasts which are generally underestimated by standard cell viability assays. A combination approach of morphological and immunolabeling methods could provide more valuable information about the toxic effect of resin monomers.

*Corresponding author
E-mail: giovanni.mazzotti@unibo.it

Meat efficiency and interior Simmental and Red-Motley Swedish bovines at fattening of low concentrates diets in conditions of intensive agriculture

VI Gudymenko, RF Kapustin*

Department of Animal Morphology, Belgorod State Agricultural Academy, Maiskii Belgorodskoi oblasti, Russia

The purpose of this work is studying of degree of display of a genotype of meat efficiency Simmental and Red-Motley Swedish bovines at limited use and absence of concentrates with introduction in their diet of the high-energy and vegetative forages prepared on special technologies. On the basis of complex experimental investigations the “know now” of a high quality beef is proved by use of genetic potential zoned import breeds on low concentrate diet in a condition of intensive breeding. Dynamism of changes and level methabolises in farding bag and in blood of animals is shown during all cycle of final fattening (180 days) at replacements in diets of grain forages by other vegetative components. The theoretical substantiation of preservation of high meat efficiency is given at rational use of grain forages that in comparative aspect is a theoretical basis at development of a work cycle intensive fattening of bovines on meat from partial and full indemnification forage fodder the forages prepared from Lucerne, Corpo and Sunflower, economic efficiency fattening of Simmental and Red-Motley Swedish bovines is determined. Real opportunities of decrease in the change of grain forages on the fattening final period (225-450 kg on one animal) are revealed.

*Corresponding author
E-mail: romankapustin@mail.ru

Feature of growth, development, meat efficiency of boviness Simmental and Limusin beeds and their hybrids

VV Gudymenko, RF Kapustin*

Department of Animal Morphology, Belgorod State Agricultural Academy, Maiskii Belgorodskoi oblasti, Russia

The purpose of work was the comparative estimation of economic-useful attributes of bovines Simmental and Limusin breeds and their hybrids. For achievement of this purpose the following tasks have been put: to determine actual consumption of forages on the period of growing of experimental animals, to study fracture of growth and development thoroughbred and hybrid bovines up to 18 monthly age, to investigate hematological parameters of young growth of genotypes, to estimate meat efficiency of bovines, qualities of meat in view of efficiency of conversion of nutrients of a forage in food efficiency, to establish optimum age of realization of bovines on meat on the basis of parameters of meat efficiency and qualitative

structure of products of slaughter, to state an economic estimation of growing of animal various genotypes till 15-18 months. In result for the first time in Central Black Soil Zone of Russia complex research of features of growth, development, meat efficiency thoroughbred and hybrid the young growth received from crossing Simmental of breed with bulls of Limusin breed is carried out. Features of formation of meat efficiency thoroughbred and hybrid bovines till 15 and 18 months are investigated. Opportunities of additional increase in manufacture of a high-quality beef are revealed due to growing Simmental-Limusin bovines. From hybrid bovines for 18 months it is in addition received 26-61 kg of a gain per one animal that provides increase in a level of profitability of production of a beef at 6,0-14,5%.

*Corresponding author
E-mail: romankapustin@mail.ru

Online teaching by an anatomy web atlas

G Halász*, Á Lukács, A Szabó, Á Szél

Laboratory of Cell and Molecular Biology, Department of Human Morphology and Developmental Biology, Semmelweis University, Budapest, Hungary

Students in the 21st century have greater and greater expectations towards the teaching quality of universities, whereas the universities, e.g.: anatomy institutes tend to provide students with broader and broader basic knowledge. Besides the lessons the role of the home study will increase. The books meet a concurrency by the wide range of anatomy study programs available on CDs or DVDs. However, similarly to the books these softwares are also static without the possibility of updating and modernizing the content. Moreover, the price of the books and softwares takes great charge on students' budget. The internet may give a solution for both problems. Our institute started to develop an online accessible anatomy web atlas called HuMo WebAtlas. As compared to other similar websites our web atlas allows not only for the passive access to dissection pictures and histology slides, but the students have the opportunity to improve and eventually even spread out the data to other students. It gives them a great chance to get involved in teaching.

Our project is based on the php 5 scripting language and uses a MySQL 4.1 database server. Thus, the development and the operation is cost-effective, because no extremely expensive softwares and investment are necessary. At the same time, owing to the independent picture and text data storing structure constructed by us, relatively small storage, memory and processor capacity are needed. The advantage is that our system can serve more users with the same resource. The content development is made easy by a user-friendly interface which is available after user authentication. Depending on the user level the system waits for supervision or transmits the changing immediately. The modular buildup ensures an easy and fast code improvement. The user interface utilizes separate dictionary database, to enable the further improvement of the currently trilingual (Hungarian, English, German) atlas. The software can store the labeling of any structure on the images that might be useful in the anatomy teaching (dissection, histology, CT, MRI, etc. pictures). Students can find the relevant information fast and easily, due to the combined thematic and keyword search scripts.

In the near future we plan to involve other related subjects such as radiology and pathology in our project to obtain an integrated database which is equally useful for students in the academic and clinical years.

Our web-atlas is accessible at <http://humo.usn.hu> with the password: "malleus" The project is sponsored by HEFOP (HEFOP-3.3.1-P.-2004-06-0014/1.0).

*Corresponding author
E-mail: halaszg@ana2.sote.hu

Undesired changes caused by long term estrogen treatment in the immunoreactivity of LH, FSH, PRL, ACTH and S-100 (present in folliculostellate cells) is modified by concomitant progesterone administration

A Heinzlmann^{1*}, M Kovács², K Köves¹

¹Department of Human Morphology and Developmental Biology, Faculty of Medicine, Semmelweis University, Budapest, Hungary, ²Department of Human Anatomy, Pécs University, Pécs, Hungary

Sexual steroids regulate the secretion of pituitary trop hormones acting directly on the pituitary gland and through the central nervous system by feed-back mechanisms. Estrogen and progesterone receptors were identified on various pituitary hormone secreting cells and in several hypothalamic and extrahypothalamic structures. In the clinical practice long term estrogen treatment is frequently applied in both male and female patients. The aim of our experiment was to study the effect of concomitant progesterone (P) administration on changes caused by long term estrogen treatment in the secretion of LH, FSH, PRL, ACTH and on the changes of S-100 (present in folliculostellate cells) immunoreactivity tested by RIA and immunohistochemistry in Sprague-Dawley male and female rats. Estrogen (diethylstilbestrol, DES) P or both in a silastic capsule were implanted under the skin of 25 day-old rats. The survival of animals were two months. The animals were decapitated in the morning, trunk blood was used for RIA and the anterior pituitary for immunohistochemistry. We have also studied whether the changed hormone secretion caused by DES can return to normal level 1 or 2 months after the removal of DES containing capsule. The following results were obtained. In the vaginal smear of female rats upon DES treatment persistent estrus was observed. DES+P did not interrupt the cyclicity but it was irregular and metestrus predominated. P alone had no effect. LH: DES depressed the basal level of LH in both female and male rats, and P did not modify the effect of DES. It was more pronounced in female than in male rats. FSH: DES and DES+P very moderately influenced the basal level of FSH in female rats and both treatment depressed it in male rats. PRL: DES dramatically enhanced the PRL levels and the effect of DES+P was much lower than that of DES alone. P did not influence the effect of treatments, in both female and male rats it showed similar tendency. ACTH: Effect of various treatment on ACTH plasma levels was very similar to their effect on the PRL levels. DES enhanced the ACTH level in both sexes, P blunted this effect. P alone did not influence the ACTH level. Immunohistochemistry supported the abovementioned results. The number of LH and FSH immunoreactive cells decreased in the anterior pituitary, the changes in the ACTH immunoreactivity was not striking, the number and the size of PRL immunoreactive cells extremely increased, they formed prolactinomas. The distribution of S-100 immunoreactive folliculostellate cells is characteristic. In intact rats these cells were evenly distributed and they formed a barrier at the border of anterior and intermediate lobes. In DES treated rats this distribution is modified. Folliculostellate cells were hardly observed inside the prolactinomas; however, these cells demarcated the prolactinomas. The effect of removal of DES capsule on the plasma hormone levels: The removal of DES capsule 2 months after implantation gradually restored the changed LH, FSH and PRL levels by the end of the succeeding 2 month survival time. Two months after removal we had results similar to the intact aged matched controls. ACTH remained higher in female rats, and in male rats it was much higher 1 month after removal and returned to intact level 2 months later. On the basis of the abovementioned results it was concluded that 1. There is sexual dimorphism in the responsiveness of gonadotropes and corticotropes to steroid treatment. 2. P blunted the enhancing effect of DES on the PRL and ACTH levels. However, its effect on the case of LH and FSH was not significant. 3. After the removal of DES its effect is partially restored. LH, FSH and PRL returned to intact level; however, ACTH remained higher by the end of 2 month survival time.

*Corresponding author
E-mail: handrea@ana2.sote.hu

The relations of the trigeminal ganglion

R Ivascu^{1*}, RI Burcin¹, A Didilescu¹, M Rusu¹, MC Niculescu², L Podoleanu¹, V Nimigean¹

¹Department of Anatomy and Embryology, Faculty of Dental Medicine, Carol Davila University of Medicine and Pharmacy, Bucharest, Romania, ²Department of Anatomy and Embriology of Medicine, Victor Babes University of Medicine and Pharmacy, Timisoara, Romania

In the middle cerebral fossa, on the antero-superior face of the petrous part of the temporal bone, near the foramen lacerum, there is the most pathological involved endocranial ganglion: trigeminal ganglion Gasser.

Observing by dissection of the macroscopic morphology of the trigeminal ganglion and its relations, represents a useful basis for the precision of the diagnosis and the efficiency of the treatment in the medical and surgical trigeminal pathology. The relations of the three main endocranial elements of the trigeminal nerve (the roots, the trigeminal ganglion and its divisions) with the vasculo-nervous elements could explain the anatomic basis of the trigeminal neuralgia.

*Corresponding author
E-mail: roxanaivascu@yahoo.com

Variants of the branches of the prescalenic part of the subclavian artery

R Ivascu*, RI Burcin, A Didilescu, R Ciuluvica, L Podoleanu, N Galie

Department of Anatomy and Embryology, Faculty of Dental Medicine, Carol Davila University of Medicine and Pharmacy, Bucharest, Romania

The first part of the subclavian artery has four branches: vertebral artery, thyrocervical trunk, internal thoracic artery and costocervical trunk. Only the thyrocervical trunk and the internal thoracic artery are the subject of different variants of origin, trajectory and branches.

To study the topography of the main variants of the thyrocervical trunk branches and internal thoracic artery.

We have studied 15 formaldehyde-prepared cadavers by dissection and macrophotography.

In 5 cases the thyrocervical trunk had three branches (inferior thyroid artery, transverse cervical artery and suprascapular artery). In 6 cases the suprascapular artery had a different origin on the second part of the subclavian artery between scalenus anterior and scalenus medius. In 3 cases the internal thoracic artery had the origin at the base of the thyrocervical trunk. In one case the thyrocervical trunk emerged from the second portion of the subclavian artery through the scalenus anterior muscle before branching in inferior thyroid artery, transverse cervical artery, suprascapular artery and internal thoracic artery.

*Corresponding author
E-mail: roxanaivascu@yahoo.com

Morphological analysis of the cloacal region in *Xenopus laevis* embryos

D Jones*, B Kramer

Embryonic Differentiation and Development Research Programme, School of Anatomical Sciences, University of the Witwatersrand, Johannesburg, South Africa

Initiation of development and differentiation of the alimentary canal involves many complex processes. The development of the cloacal region in particular, is not well understood and abnormalities in this region result in a variety of anorectal malformations, which are disabling for the newborn. The amphibian alimentary canal, a useful developmental model, develops in three parts: stomodeum, mesenteron and proctodeum. The stomodeum and proctodeum develop at the extreme anterior and posterior regions of the embryo respectively, and are the only two areas in the developing embryo where the ectodermal and endodermal germ layers are directly juxtaposed without intervening mesoderm. Molecular studies have been conducted involving the proctodeal region. However, morphological analysis of this region appears to be limited in the current literature. This study aims to investigate and elucidate morphological features present during the development of the proctodeal region and dissolution of the cloacal membrane in *Xenopus laevis* embryos. *Xenopus laevis* frogs were mated and the resulting embryos were collected, allowed to develop further in a suitable environment and staged according to Nieuwkoop and Faber (1967). For all the techniques used, a minimum of six specimens at each stage were analysed. Staged specimens were fixed in 10% formalin, routinely processed and embedded in JB-4 resin for histological evaluation. Serial sections were cut at 6µm and stained with Gill's haematoxylin and eosin technique, to examine the general structure and pin-point dissolution of the cloacal membrane. Confocal microscopy was used for optical fluorescent sectioning to view interior structures. Specimens for confocal microscopy were fixed in Bouin's fixative. For scanning electron microscopy, embryos were fixed in 2.5% glutaraldehyde, post-fixed in 1% osmium tetroxide and routinely processed. Three dimensional images of the proctodeal region were obtained using the scanning electron microscope. Initially at the caudal end of the embryo, the ectoderm invaginates (stage 21) forming a small depression, known as the proctodeum. There is apposition of the outer ectoderm and inner endoderm. Low cilia are found dispersed evenly across the surface of the embryo. As development continues, from stage 21 to stage 23, the ectodermal depression deepens and the ectoderm and endoderm become reduced in thickness to form the cloacal membrane. The cells around the proctodeum project out forming a slight bulge. The cilia become more numerous and appear more concentrated around the anal region. The depression increases and at stage 24 there is perforation of the membrane, producing a free passage of communication from the hindgut to the exterior. From stage 24 to stage 26 the perforation increases in width and becomes more apparent. Molecular analysis of this region is ongoing. Morphological evidence combined with molecular analysis will provide a greater understanding of the development of the proctodeal region and dissolution of the cloacal membrane.

Nieuwkoop PD, Faber J (1967) Normal Table of *Xenopus laevis* (Daudin): A systematical and Chronological survey of the Development from the fertilized egg till the end of metamorphosis. Eds. North-Holland Publishing Company, Amsterdam.

*Corresponding author
E-mail: dmjones99@gmail.com

Clinical histology of liver of cattle newborn calves: applied aspect of study

RF Kapustin*, RV Romenskiy

Department of Animal Morphology, Belgorod State Agricultural Academy, Maiskii Belgorodskoi oblasti, Russia

The aim of given research is to determine diagnostic significance of morphological monitoring at newborn calves with liver diseases. Liver plays a very important homeostatic function, besides it has considerable stock of reserve potential (cubic content), that causes objective difficulties in timely diagnostics, definition of nosologic belonging to its damages and formulation of prognosis. Liver diseases can take their course latently, asymptotically for a long time, causing great damage to organism overall. Especially it is actual for newborn animals. Imperfection of compensation and adaptation mechanisms in early age causes development of severe complications. Therefore, timely diagnostics of liver affections will allow raising the quality of veterinary measures greatly. Researches have been done in newborn calves of cattle with observation of rules of works conducting with the use of experimental animals. In this process we determined clinical status and carried out laboratory examination of blood with definition of some hematological and biochemical indexes. Laboratory tests included erythrocytes quantity, leukocytes quantity, haemoglobin quantity, rate of erythrocyte sedimentation and leukocytic formula; total protein, protein fractions, trial on colloidal stability of plasmatic proteins, immunoglobulin sum in blood serum, activity of transaminases. It has been determined, that liver affections of young stock are accompanied by unspecific deviations from clinical status, such as hypothermia, tachycardia and « polypnoe». Changes in circulating blood were characterized by traits of hypoplastic anaemia, hypo- and dysproteinemia with violation of colloidal stability of plasmatic proteins and low activity of indicator enzymes (glutamic-alanine transaminase, glutamic-aspartic transaminase). The violations of functional condition of liver at newborn calves of cattle are characterized by absence of display of strongly pronounced specific pathological traits, and the use of means of laboratory diagnostics, as a rule, doesn't allow to determine nosologic belonging to disease, because states only violation of function but not structural violation. Based on data received we have done a device for puncture biopsy (patent RU 49705 U1), allowing to carry out early diagnostics of structural damages of liver at newborn calves of cattle. Received biopsy material has been processed with the help of methods of classical histotechnics, and it has been revealed that structural changes of liver have been followed by unformed liver structures, sharp reduction of quantity of binuclear hepatocytes, availability of fields of destructively changed cells with phenomena of caryolysis and macrophagous reaction. We can mention also: nucleus polymorphism, availability of hyperchromatic nuclei in hepatocytes, centers of micro- and macronecrosis. There were parts of hemopoietic active tissue in sinusoidal areas. Thus, morphological monitoring of liver plays a very important part in differential diagnostics and formulation of prognosis at diseases of hepatobiliary system of different genesis.

*Corresponding author
E-mail: romankapustin@mail.ru

The influence of rabbits outbreeding as on hair integument and as on quality of insipid-dry coats (fells)

RF Kapustin*, NS Trubchaninova, VP Trubchaninova

Department of Animal Morphology, Belgorod State Agricultural Academy, Maiskii Belgorodskoi oblasti, Russia

Our aim was to study of hair quality and fells of cross-breeds F1 and F2 during outbreeding and the comparison of got data with breed of same age of unitial breeds. In order to get this aim we study morphometris and histological index of skin-hair integument of breeds and cross-breeds animals. The study objects were breeds of rabbits: Silver rabbits, New Zealand white, Vienna blue, White giant and their cross-breeds. The groups were formed according to princip of balanced group-analogue, with polygamy correlation 1:5. The skin integument length, thickness and density were studied by method of comparative analysis of rabbits breeds and cross-breeds from 30 to 180 days age. The insipid-dry feels were studied during different age periods according to species, size and differeness. During our study the trastworthy differentce of insipid-dry fells quality was noted (cross-breeds animals fells with higher quality). It is caused by skin thickness increase of alive animals, nippe layer of dermal with decreased thickness of epidermis. We have found: a) he higher density of roots disposition of beard hair; b) decrease of roots buns area of down hair. The cross-breeds animals have less length of all hair kinds, than breeds have. Cross-breed rabbits (on comparison with breed rabbits) had more density and aqualize on density of hair integument, more over, the breeds animals length of all hair integument is more. Thuse, cross breeding rabbits F1 and F2 exceed the breed animals of same age on skin-hair integument quality of all index.

To get rabbits high quality fells is important reserve of rabbit breeding. As well as, the skin condition and hair shows the level of rabbits health and constitution strenght. Our aim was to study of hair quality and fells of cross-breeds F1 and F2 during outbreeding and the comparison of got data with breed of same age of unitial breeds. In order to get this aim we study morphometris and histological index of skin-hair integument of breeds and cross-breeds animals. The study objects were breeds of rabbits: Silver rabbits, New Zealand white, Vienna blue, White giant and their cross-breeds. The groups were formed according to princip of balanced group-analogue, with polygamy correlation 1:5. The skin integument length, thickness and density were studied by method of comparative analysis of rabbits breeds and cross-breeds from 30 to 180 days age. The insipid-dry feels were studied during different age periods according to species, size and differeness. It is supposed, that cross-breeds animals show shorter period of age shedding of hair, as well as the skin constitution changes, causing the density rigsen, equalization of hair integument density, the quality and size improvement of insipid-dry fell. During our study the trastworthy differentce of insipid-dry fells quality was noted (cross-breeds animals fells with higher quality). It is caused by skin thickness increase of alive animals, nippe layer of dermal with decreased thickness of epidermis. We have found: a) he higher density of roots disposition of beard hair; b) decrease of roots buns area of down hair. The cross-breeds animals have less length of all hair kinds, than breeds have. Cross-breed rabbits (on comparison with breed rabbits) had more density and aqualize on density of hair integument, more over, the breeds animals length of all hair integument is more. Thuse, cross breeding rabbits F1 and F2 exceed the breed animals of same age on skin-hair integument quality of all index.

*Corresponding author
E-mail: romankapustin@mail.ru

The surgical anatomy of the biliary tree for living donor liver transplantation

M Kiss^{1,2*}, S Kovács¹, K Gorove¹, L Kóbori², K Törő¹, I Kristóf³, Á Nemeskéri¹

¹Department of Human Morphology and Developmental Biology, Semmelweis University, Budapest, Hungary,

²Transplantation and Surgical Clinic, Semmelweis University, Budapest, Hungary, ³Department of Forensic Medicine, Semmelweis University, Budapest, Hungary

In 1963 Starzl performed the first successful human liver transplantation. Nowadays it is a routine operation. The shortage of cadaveric organs has led to the development of partial living donor liver transplantation (LDLT). LDLT in children uses the left lateral lobe (segment II and III). To avoid small-for-size graft syndromes in adult patients, many centres use right-lobe grafts. Right-lobe LDLT has become an important therapeutic option for adult patients suffering from end-stage liver disease. Different series have shown encouraging results, reporting 1-year graft and patient survival rates of up to 80% (Marcos 2000; Miller et al. 2001). Nevertheless, right-lobe LDLT still represents a challenging surgical procedure in which the donor's safety must be paramount. The basis of the LDLT is the detailed knowledge of variations in segmental anatomy and the ramifications involving the portal and hepatic venous systems, and hepatic ducts. We designed a new synthetic resin corrosion cast method in order to study these variations. Two years ago in Belgrade we presented the arterial blood supply of liver segments, showing important anastomoses between liver segments and portal variations made by our new method. Smadja and Blumgart (1994) have classified the biliary variations into six main types. The variations in the anatomy of intrahepatic bile ducts also complicate operations in LDLT (biliary complication rates are between 10 to 20 per cent in the ex situ partial liver transplantation (Rogiers et al. 2002). Therefore, the aim of the last two years of research was to examine these variations of the biliary tree based on our new synthetic resin corrosion cast method. Until now 30 biliary corrosion casts have been prepared. We found a normal variation (type A) in 19 preparations (63,33%). In 7 preparations (23,33%), there is an aberrant drainage of the right segmental ducts (right posterior or right anterior hepatic ducts) into the left hepatic duct. In one of these preparations (3,33%) the right anterior hepatic duct fused with the left hepatic duct, the right posterior hepatic duct fused with the cystic duct, and the resulting two ducts fused to form the "bile duct". In another preparation, the right anterior hepatic duct fuses with left, and the right posterior hepatic duct drains into this common duct 15 mm below the confluence and 16 mm above the cystic duct's entry. Conclusion: The branching pattern of intrahepatic biliary tree was atypical in 36,66% of cases. Since the biliary complication (biliary leakage and stenosis) remains a major cause of morbidity after liver transplantation, the knowledge of the biliary variants is essential for the successful surgical management of LDLT.

Miller CM, Gondolesi GE, Florman S, Matsumoto C, Munoz L, Yoshizumi T, Artis T, Fishbein TM, Sheiner PA, Kim-Schluger L, Schiano T, Shneider BL, Emre S, Schwartz ME (2001) One hundred nine living donor liver transplants in adults and children: a single-center experience. *Ann Surg* 234(3):311-312.

Marcos A (2000) Right-lobe living donor liver transplantation. *Liver Transpl* 6(Suppl2): S59-63.

Rogiers X, Bismuth H, Busuttill RW, Broering DC, Azoulay D (2002) Split liver transplantation. Steinkopff-Verlag, Darmstadt.

Smadja C, Blumgart LH (1994) The biliary tract and the anatomy of biliary exposure. In Blumgart LH, Ed. *Surgery of the Liver and Biliary Tract*. Vol. 1. 2nd Ed. Edinburgh: Churchill Livingstone, pp. 11-24.

*Corresponding author

E-mail: kissmatyas@gmail.com

Expression of a novel isoform of BEN-like antibody produced against guinea fowl's bursal cells

K Kocsis*, É Bíró, N Nagy, I Oláh

Department of Human Morphology and Developmental Biology, Semmelweis University, Budapest, Hungary

A panel of monoclonal antibodies (mAb) was raised against non-fractionated bursal cells to produce anti B cell specific marker. Cell suspension was prepared from bursa of Fabricius of guinea fowl, which contained more than 90% of lymphocytes and few percents of epithelial cells. The supernatants of hybridomas were tested immunocytochemically on adult and embryonic tissues and cloned to select monoclonals.

In recent work we present one of the mAbs, which recognizes highly different tissues during embryonic development suggesting that the expression of this antigen is developmentally regulated and cross-reacts with chicken tissues. In adult bursa of Fabricius of the chicken this mAb designated NAKO recognizes every epithelial components except follicle-associated epithelium. The gut epithelium after closing entoderm is transiently positive. The transient antigen expression emerges first in the notochord of embryonic day (ED) 2 and by day five ceases, when the cells of the sclerotom, which appeared around the notochord begin to express it. DE3 and 4 the dermomyotome also expresses the NAKO positive antigen. Soon after the notochord at 3 DE the floor plate of the neural tube becomes positive, which is followed by the expression of basal plate where the motoneurons differentiate. Outgrowing axons of the motoneurons also express the antigen. Strong NAKO positivity characterizes the spinal sensory ganglions and their central and peripheral processes. By day 5DE the developing intestinal plexus is highly positive. The expression of this antigen continues after hatching on all parts of the peripheral nervous system. In the splanchnic mesenchyme of the ventral part of the embryo strong transient NAKO reaction appears which ceases around 10 DE. On the extraembryonic membranes (amnion) the antigen also appears unlike the ectoderm.

Summarizing the antigen expression we can conclude: In the peripheral nervous system the antigen expression is maintained after hatching, while in the mesoderm- and endoderm- derived structures is transient. The molecular weight and the major immunohistochemical features of the NAKO highly similar to the BEN/SCI/DM-GRASP antibodies (Pourquie et al. 1990; Pourquie et al. 1992; Corbel et al. 1996). Thus the NAKO identified molecule could be a homologue molecule to the BEN. Because the NAKO mAb was produced against guinea fowl cells, not chicken cells and it works in both species, suggests that this molecule is highly conservative. This was confirmed, that homologue molecules were found in fish, rat and human. The NAKO might be a novel isoform molecule of the BEN because its expression differs from it in several tissues *i.e.* cardiac septum and ventral and splanchnic mesenchyme where the cell adhesion function of the NAKO is questionable.

Corbel C, Pourquie O, Cormier F, Vaigot P, Le Douarin NM (1996) BEN/SCI/DM-GRASP, a homophilic adhesion molecule, is required for in vitro myeloid colony formation by avian hemopoietic progenitors. *Proc Natl Acad Sci USA* 93:2844-2849.

Pourquie O, Coltey M, Thomas JL, Le Douarin NM (1990) A widely distributed antigen developmentally regulated in the nervous system. *Development* 109:743-752.

Pourquie O, Corbel C, Le Caer JP, Rossier J, Le Douarin NM (1992) BEN, a surface glycoprotein of the immunoglobulin superfamily, is expressed in a variety of developing systems. *Proc Natl Acad Sci USA* 89:5261-5265.

*Corresponding author
E-mail: kkocsis@ana2.sote.hu

Trabecular gel network capable of phase transition may exist in brain neurons

B Kovács*, F Gallyas

Department of Neurosurgery, University of Pécs, Pécs, Hungary

In the course of many neurological diseases, individual non-apoptotic neurons randomly distributed among undamaged neurons become dramatically shrunken, hyperbasophilic and argyrophilic („dark” neurons). The shrinkage is caused by a potentially reversible, striking reduction of all distances between undamaged ultrastructural elements (compaction), which is accompanied by the escape of the excess water through visibly intact plasma membrane into adjacent astrocytes. The same ultrastructural compaction can also be produced by momentary physical forces, such as head injury and electric shock, even under post-mortem circumstances that are extremely unfavorable for enzyme-mediated biochemical processes. From this, we (Gallyas et al. 2004) concluded that the ultrastructural compaction consists in a pure physical phenomenon.

It is known from polymer chemistry (Annaka and Tanaka, 1992) that certain synthetic gels can have two or more metastable phases, each having a discrete minimum of non-covalent free energy, a discrete set of conformations of the macromolecules constituting the gel matrix, a discrete water content (and therefore a discrete volume), and also a discrete set of physical and chemical properties. Initiated at a single point, transition from one gel phase to another, the essence of which is a cooperative conformational change in the macromolecules constituting the gel matrix, can spread throughout the whole gel volume, propelled on the domino principle by the difference in non-covalent free energy. The initiation can be brought about by a subtle change around a critical concentration of various chemical substances or a critical degree of various physical forces, and was assumed to comprise the central mechanism in most cell functions in which mechanical work is involved (reviewed by Pollack 2001).

By analogy with the above physicochemical phenomenon, we (Gallyas et al. 2004) deduced from several enigmatic phenomena concerning the “dark” neurons that the morphological substratum of the dramatic compaction of the ultrastructural elements is a ubiquitous intracellular gel structure capable of spreading phase transition at the expense of stored non-covalent free energy. In a recent paper we (Kovács et al. 2007) raised the idea that this gel structure does not fill completely and evenly the spaces between the ultrastructural elements, but exists in the form of an unbroken network of interconnecting trabeculae embedded in a confluent system of lacunae filled with fluid cytoplasm. Through these lacunae water molecules can rapidly reach the plasma membrane from any point of the cell, resulting in the same degree of compaction both in the core and the periphery of the affected neurons. Furthermore, this idea can reconcile the membrane-derived properties (e.g. ion channels) with gel-derived properties (see Pollack 2001). Finally, this trabecular gel network might be the *in-vivo* (unfixed) equivalent of the strongly criticized microtrabecular lattice demonstrated in aldehyde-fixed and subsequently freeze-dried cells in the high-voltage stereo electron microscope, and interpreted as a “solid” component of the cytoskeleton (reviewed by Porter 1989). By gradually forming covalent bonds, aldehyde fixation stabilizes the energy-storing phase of the trabecular gel structure.

Annaka M, Tanaka T (1992) Multiple phases of polymer gels. *Nature* 355:430-432.

Gallyas F, Farkas, O, Mázló M (2004) Gel-to-gel phase transition may occur in mammalian cells: Mechanism of formation of “dark” (compacted) neurons. *Biol Cell* 96:313-324.

Kovács B, Bukovics P, Gallyas F (2007) Morphological effects of transcardially perfused sodium dodecylsulfate on the rat brain: Cell-biologic aspects. *Biol Cell* (in press). doi:10.1042/BC20060128.

Pollack GH (2001) *Cells, Gels and the Engines of Life*. pp. 1-298, Ebner and Sons, Seattle.

Porter KR (1989) The cytoplasm and its matrix. *Prog Clin Biol Res* 295:15-20.

*Corresponding author

E-mail: fiona55@freemail.hu

Both embryonic and adult stem cells give rise to endodermal derivatives such as cells of the pancreas and liver

B Kramer

Embryonic Differentiation and Development Research Programme, School of Anatomical Sciences, Faculty of Health Sciences, University of the Witwatersrand, Johannesburg, South Africa

Undifferentiated cells which self-renew and produce functionally specialized cells are termed stem cells. Because of their potential in regenerative medicine, both embryonic stem cells, which are pluripotent, and adult stem cells, which are multipotent, are being utilized for cellular therapy. Embryonic stem cells differentiate spontaneously into many cell types including those of the haemopoietic system (Evans and Kaufman 1981) and the myocardium. Adult stem cells were thought to possess a very limited potential to differentiate into other cell types, but have recently been shown to differentiate into skeletal and cardiac muscle fibres, renal tubular epithelial cells and neurones. This paper will describe how both embryonic stem cells and adult stem cells are capable of giving rise to cells of the liver and pancreas.

In experiments utilizing mouse embryonic stem cells, embryoid bodies (EBs) were cultured with quail mesoderm of the dorsal pancreatic bud (Hamilton and Hamburger stage 25) to determine whether insulin- and glucagon-containing cells could be induced. Quail mesoderm was used so as to be able to identify the origin of the resulting endocrine cells. The explants were cultured for 7 days in Matrigel in the wells of a Nunclon multidish in serum-free Ham's F12.ITS culture medium at 37°C in 5% CO₂ in air. The explants were freeze dried, fixed in parabenzoquinone vapour and embedded in epon araldite resin. Insulin- and glucagon-immunofluorescence were detected in groups of cells within the EBs, indicating that EBs can generate both α - and β -cells in the presence of signalling molecules from pancreatic mesoderm.

In the second experiment*, bone marrow cells were harvested from the femurs of adult male mice (CBA) and injected into the tail vein of 6 week-old female mice (CBA), which had undergone whole-body gamma irradiation. After 11 weeks, four female mice were killed and a further six were killed 30 weeks post-transplantation. The liver and pancreata of the mice were removed, fixed in 10% buffered formalin for 24hrs, processed and embedded in paraffin wax, followed by serial sectioning at 4 μ m. Serial sections of tissue 16 μ m apart were selected for labelling. An *in situ* hybridisation method, for labeling the Y-chromosome of cells originating from male mice, was utilized. Y-chromosomes, identified by the use of the chromogen DAB, were identified in liver and pancreatic tissue. While only a few cells were found to be Y-chromosome-positive in the liver of female mice, substantially more Y-chromosome-positive cells were present in the pancreas. In addition, the tissue of mice killed 30 weeks after transplantation appeared to contain more male-derived cells than did the tissue of mice killed 11 weeks after transplantation.

The putative signaling molecules controlling the differentiation of these stem cells into functional cell types will be reviewed.

*Experiment carried out in collaboration with D Brynmor Thomas, A Riches and T Briscoe, School of Biological Sciences, University of St. Andrews, Scotland and A Marais, School of Anatomical Sciences, University of the Witwatersrand.

Evans M, Kaufmann MH (1981) Establishment in culture of pluripotential cells from mouse embryos. *Nature* 292:154-155.

E-mail: Beverley.kramer@wits.ac.za

Changeability dynamics of basic anthropometric indexes of newborn children from regions with different ecological situations

EN Krikun¹, VV Boldyr¹, RF Kapustin^{2*}, IA Zinchenko¹

¹Department of Human Anatomy and Histology, Belgorod State University, Belgorod, Russia, ²Department of Animal Morphology, Belgorod State Agricultural Academy, Maiskii Belgorodskoi oblasti, Russia

We have carried out the research on revealing of changeability of main morph - functional indexes of newborn children in dependence on ecological situation in regions of their mothers living from 1973 to 2004. Statistical analysis of morph - functional indexes of newborn children by individual traits in dependence on ecological situation in regions of their birth and their mothers living has shown that body dimensions of newborn boys from regions with critical ecological situations (ESC) have no accident greater mean values as compared with newborn boys from regions with satisfactory ecological situations (ESS). Their body mass is greater by 90 grams ($p < 0,001$), head circumference - by 0,33 centimeter ($p < 0,001$), chest circumference - by 0,46 centimeter ($p < 0,001$). These children give in insignificantly to newborn boys from regions with tense ecological situation (EST) in erythrocytes level. Other traits have not given any essential differences. The results of dispersion analyses of some morph – functional traits of newborn girls in dependence on ecological situation testify to no accident character of differences in indexes of circumferences of head and chest, and in level of Apgar trait. So, average levels of head circumference of newborn girls from ESC regions are greater by 0,25 centimeter as compared with newborn girls from EST regions ($p < 0,01$). These children have greater average levels of chest circumference as compared with children from EST and ESS regions by 0,26 centimeter accordingly ($p = 0,001$). Average level of their functional condition on Apgar scale is lower (by 0,25 points) as compared with children from ESS regions, but this index doesn't deviate from the framework of normal value ($p < 0,01$). Degree of multidimensional differences of children's groups from regions with various ecological situations by complexes of traits has been measured with the help of distances of Mahalanobis with calculation for them value of F-criterion. The results of investigations have shown that during the period from 1973 to 2004 the dynamics of intergroup changeability of basic anthropometric indexes of newborn children is characterized by insignificant increase of their mean values in regions with critical ecological situation in an interval from 1973 to 1985. By the end of XX century mean values of these characteristics of newborn children from regions with various ecological situations have become smooth. This fact can be explained by reduction of anthropogenic loading in a period from 1985 to 2000 in connection with common economic fall of production.

*Corresponding author
E-mail: romankapustin@mail.ru

The morphology of immune competent organs in neonatal productive animals

B Krishtoforova, V Lemeshchenko*

Chair of Anatomy and Physiology of Animals, Southern branch "Crimean Agrotechnological University" of National Agricultural University, Simferopol, Ukraine

The birth of animals with low viability occur in contemporary conditions that is conformed by their diseases with frequent lethal result, on their first days of life. The prenatal underdevelopment, owing to breach placental barrier, is the basic cause of lowering of the natural resistance in neonatal animals (Vodel 1977; Хрусталева 1995; Левченко, Надточій 1998; Грабчак 2000; Даньків 2002). The aim of our researches is to determine the morphology peculiarities of immune competent organs in neonatal calves and piglets. We had investigated immune competent structures (the organs of universal hemo-and-immunopoiesis and also lymphocytopoiesis) in one day old calves ($n=15$) and piglets ($n=15$), using the complex of methods: anatomical preparation, X-ray method, microscopy of hystological preparations and statistic. The result of our research is following. The immune competent organs were determined on the anatomical level in neonatal animals. Diaphysal and epiphysal hearths of ossification were exposed into the organs of universal hemo-and-immunopoiesis (bone organs) by X-ray method in both

calves and piglets. The apophysal ones are typical for long tubular bone organs of extremities in calves and it is absent in piglets. The formation of bone tissue is the result of endesmal and enchondral ossification in one day old calves and piglets. The endesmal osteogenesis occur in diaphysis of the long tubular bones. Compact bone tissue is of smesh structure, and connective tissue, blood vessels and nerves are disposed in its cells. The spongy bone tissue is formed by enchondral osteogenesis but red bone marrow, realizing function of universal hemo-and-immunopoiesis, is situated in its cells. Anatomically thymus possesses pair and impair cervical lobes and also impair thoracal ones in the neonatal calves and piglets, but its absolute mass is 105.0-175.0 g, relative one is 0.5-0.75% in calves. The cortical-and-medullar ratio constitutes 1:2 or 1:3 in thymical lobules. In neonatal animals the spleen is also anatomically formed. Parenchime of the spleen is formed by red pulp (75.5%-88.5%) and white one or diffusive and nodular lymphoid tissue (7.5%-12.3%). The individual splenic lymphoid nodules have germenative centers. That is the evidence of their particular functional activity. It should be noted, the analogeous lymphoid nodule (with germenative centers) is formed in limphatic knots, especially in visceral ones, but also in limphoid structure associating with mucosal cover of digestive organs in developed neonatal calves and piglets. Thus on anatomical and tissue levels the immune competent organs are characterized by some incompleteness in neonatal maturity animals. However they are able to react, to a certain degree, on the influence of genetic alien agents that is confirmed by the presence of the lymphoid nodule with germenative centres.

Грабчак ЖГ (2000) Морфофункціональний статус органів універсального гемопоезу у неонатальних телят. Вісник БДАУ, Біла Церква 13:2-63-67.

Даньків ОМ (2002) Імунний статус плодів і телят з різним антенатальним розвитком : Автореф. дис. ... канд. с/г наук : 03.00.13. Львівська ДАВМ ім. С.З. Гжицького. Львів.-20.

Левченко ВІ, Надточій ВП (1998) Антенатальна гіпотрофія телят. Ветеринарна медицина України. 8:38-40.

Хрусталева ІВ (1995) Морфофункціональний статус и тесты его определяющие у млекопитающих и птиц. Морфофункціональний статус млекопитающих и птиц: Тр. науч. конф. морфологов: Симферополь.-3.

Vodel M (1977) Morphologische Placenta befunde bei fetuler Hypo- und Hypertrophie. Z Geburts und Perinat 8:45-52.

*Corresponding author

E-mail: lemeshenko@mail.ru

Structural-and-functional peculiarities of hepatic veins and components of tissue in piglets of neonatal period

B Krishtoforova, V Lemeshchenko*

Chair of Anatomy and Physiology of Animals, Southern branch "Crimean Agrotechnological University" of National Agricultural University, Simferopol, Ukraine

The liver in mammals is a poly functional organ, developing in a prenatal period of ontogenesis as a structural component of the digestive apparatus and in a postnatal period of development adopting the function of «metabolic brain» of the organism (Розен и др 1991). The liver of a new-born human and immaturity mammals (white rats) remains the certain uncompleteness of structure, that can be observed in the absence of classic structure lobules, saved hearths of hemopoiesis and temporary vascular formations (umbilical vein and venous duct), associating with the organ. Research, devoted structural features and morphogenesis of vascular and tissue components of liver in neonatal period piglets, are occasional (Смирнова 1967; Kaman 1968). The purpose of our research is to set the stuctural-and-functional peculiarities of hepatic veins and components of tissue in piglets of neonatal period. Afferential and efferential veins, stromal and parenchimal components of the liver were determined in 1-20 days old piglets, using the morphological, X-ray anatomical and statistical methods. The results of research are following. Afferential (umbilical and portal) and efferential (caudal cava and hepatic) veins form afferential and efferential collectors accordingly. They regulate the intensity of intraorganical blood flow and volume of blood current to the heart from the abdominal region in one day old piglets. They do not only communicate by sinusoids of "rete mirabile" in parenchime of the organ but also by means of plural portal-and-caval anastomosis, which are the analogues of venous duct (Fig. 1). The parenchime of the liver has a spongy structure in one day old piglets. Hepatocytes form the ramified beams, sinusoids and shallow hemopoietic hearths are disposed among them. The lobules of classic structure are not found in the liver. The umbilical vein almost fully was obliterated in 10 day's old piglets, saving a narrow, winding road clearance for certain animals, and

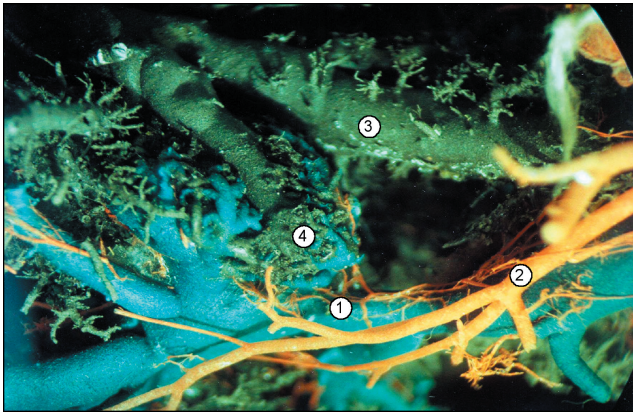


Figure 1. Corrosion preparation of the hepatic blood vessels of a one day old piglet. 1 – afferential collector; 2 – hepatic artery; 3 – caudal cava vein (efferential collector); 4 – plural portal-and-caval anastomosis.

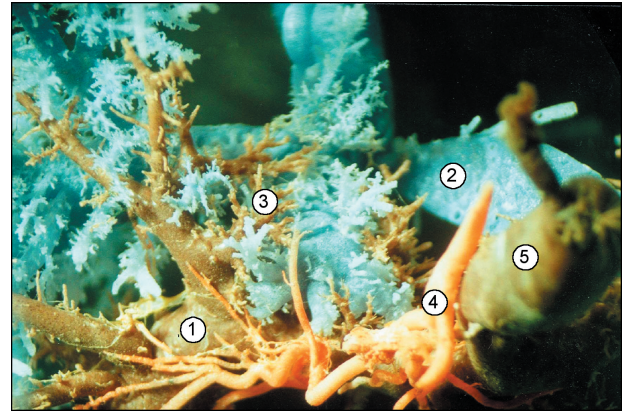


Figure 2. Corrosion preparation of the hepatic blood vessels of a 20 day old piglet. 1 – afferential collector; 2 – caudal cava vein (efferential collector); 3 – postanastomotic branches; 4 – portal vein.

plural portal-and-caval anastomosis is transformed in shallow intraorganical veins on the border of the caudal and left lateral lobes of liver. The coiled and long capillaries are disposed among such veins. The lobules of primitive structure are formed in parenchime of the organ, not having expressed scopes with each other (50.3%), and also lobules are formed with clear scopes from septal connecting tissue (28.6%). The parenchime of spongy structure (21.1%) is saved mainly in the subcapsular area of the liver. The hearths of hemopoiesis are not found out in thr hepatic parenchime. The 20 days old piglets have complete obliteration of temporary anastomotic veins; the sinusoidal network, incident to the other areas of the hepatic parenchime, is formed between afferential and efferential veins in the location area of the plural portal-and-caval anastomosis in one day old piglets. The anastomosis become short treelike veins (Fig. 2). The lobules of the completed structure (59.6%) predominate above primitive ones (40.0%) in parenchime of the liver. The spongy parenchime only saves 0.4%. Thus the hepatic blood vessels and tissue components are characterized by the stuctural-and-functional uncompleteness in accordance with the degree of the organism maturity of animals. Obliteration of the temporary hepatic veins in piglets during their neonatal period on the background of forming the lobules in the parenchime of classic structure, and the disappearance of hemopoietic hearths. To our opinion, it is related with settling the definitive functions of the organ.

Розен ВВ и др. (1991) Половая дифференцировка функций печени. М.: Медицина.–336.

Смирнова ЮГ (1967) О кроветворении свиней после рождения. С.-х. биология. 2:2.–316-318.

Kaman J (1968) Der Umbau des Ductus Venosus beim Schwein. II. Posnatales Stadium. Anat. Anz.122:5.–476-486.

*Corresponding author
E-mail: lemeshenko@mail.ru

Fractal organisation of tissue growth patterns in canine trichoblastomas

GA Losa^{1*}, G De Vico^{2*}

¹Institute of Scientific Interdisciplinary Studies, Locarno, Switzerland, ²Department of Biological Sciences, Faculty of MM,FF,NN Sciences, University Federico II, Napoli, Italy

Canine Trichoblastoma are hair follicle tumours of different subtype constituted by epithelial component (hair germ) and mesenchymal component (dermal papilla) which closely interact. The architecture and the epithelial growth patterns of the different histological subtypes, namely Ribbon type, Trabecular type, Granular Cell type and Spindle cell type, were cha-

acterised by fractal analysis (Mandelbrot 1983) and conventional morphometry. The architecture and the epithelial growth patterns of the different subtypes were characterised by fractal analysis. The Fractal Dimension (FD) was determined from the slope of the regression line describing the fractal region within the bi-asymptotic curve experimentally established by means of the FANAL++ software (Losa and Nonnenmacher 1996). The FD obtained from masks and outlines after grey threshold segmentation of tumour epithelial components showed self-similar fractal properties. Masks but not outlines of canine trichoblastoma subtypes showed significant different FD values ranging from 1.75 to 1.85 thus enabling a complete discrimination of different histological types. Trichoblastoma subtype with the higher amount of mesenchymal stroma (Losa and Alini 1993) displayed an epithelial component with the lowest FD, indicative of less complex growth patterns. The FD data suggest that an iterative morphogenetic process, involving both the hair germ and the associated dermal papilla, may be responsible for the tumour architecture (De Vico et al 2005) and emphasizes the advantages of fractal analysis in the objective characterization of tumour growth.

Mandelbrot BB (1983) *The fractal Geometry of Nature*. Freeman, San Francisco.

Losa GA, Alini M (1993) Sulfated proteoglycans in the extracellular matrix of human breast tissues with infiltrating carcinoma. *Int J Cancer* 54:552-557.

Losa GA, Nonnenmacher TF (1996) Self-Similarity and fractal irregularity in pathologic tissues. *Modern Pathol* 9(3):174-182.

De Vico G, Peretti V, Losa GA (2005) Fractal organization of feline oocyte cytoplasm. *Eur J Histochem* 49(2):151-15.

*Corresponding authors

E-mail: glosa@cerfim.ch; gionata.devico@unina.it

Photopigment coexpression in the mammalian retina

Á Lukáts*, A Szabó, G Halász, Á Berta, P Röhlich, V Doma, D Végvári, Á Szél

Department of Human Morphology and Developmental Biology, Semmelweis University, Budapest, Hungary

In mammals, each cone had been thought to contain only one single type of photopigment. It was not until the early 1990s that photopigment coexpression (dual cones) was first reported. In a well known laboratory animal, the house mouse, the distribution of color cones shows a characteristic division. Whereas in the upper retinal field the ratio of short wave to middle-to-long wave cones falls in the usual range (1:10), in the ventral retinal field M/L-pigment expression is completely missing. In the transitional zone, numerous dual cones are detectable (spatial photopigment coexpression). In some other species without retinal division, dual cones appear during development, suggesting that M/L-cones develop from S-cones. Dual elements represent a transitory stage in M/L-cone differentiation, and disappear with maturation (transdifferentiation, transitory photopigment coexpression). These two phenomena seem to be mutually exclusive in the species studied so far.

Recent comparative studies performed by our group reported other types of retinal photopigment coexpressions in adult specimens without retinal division. Dual elements either occupy the dorsal peripheral retina, or make up the entire cone population.

In an African diurnal rodent, *Otomys unisulcatus*, a few dual cones appear in peripheral localization. These cones morphologically resemble developing elements raising the question as to whether these are postmitotic cells in the phase of differentiation. Strong immunoreactivity against PCNA (Proliferating Cell Nuclear Antigen) in this region suggests that, at least in this species, retinal maturation or regeneration continues even in adults. Intensive studies are on the way to detect a similar phenomenon amongst available laboratory animals.

In two of the examined species, the Siberian hamster, and the African pouched mouse the entire cone population is made up of dual elements. This is the first observation proving that all cones of a retina are of dual nature. These species are good models for the study of molecular control of opsin expression and renders them suitable sources of dual cones for investigations on the role and neural connections of this peculiar cone type.

In the developmental studies performed, the retinal maturation of several species was examined to test the hypothesis of transdifferentiation. Whereas in all species studied, S-pigment expression, if present, precedes that of the M/L-pigment, dual cones are not always detectable. They are either present in a smaller or larger number or are completely missing from the

developing retina. These results exclude a common mechanism for M/L-cone maturation: they either transdifferentiate from S-cones or may develop independently.

The experiments have been supported by the following grants: Hungarian Scientific Research Fund (OTKA #T-042524, #F-61717).

*Corresponding author
E-mail: lukats@ana2.sote.hu

The effect of TGF- β 1 and high glucose on the development of insulin cells in the chick pancreas

A Marais*, PT Govan-Shiba, B Kramer

Embryonic Differentiation and Development Research Programme, School of Anatomical Sciences, University of the Witwatersrand, Johannesburg, South Africa

Numerous factors are believed to affect the proliferation and differentiation of β -cells, which are responsible for secreting insulin in the pancreas. A means of enhancing β -cell proliferation in the pancreas would prove invaluable in the treatment of insulin-dependant diabetes. TGF- β 1 is thought to decrease the proportion of β -cells with respect to α -cells, while glucose is thought to enhance β -cell proportions in rats (De Gasparo et al. 1978). However, recent studies have shown that chick pancreatic cells may respond differently to glucose by showing a reduction in β -cell proportions (Kramer and Alison 2005). Long-term exposure to glucose has also been shown to have an apparent inhibitory effect on β -cells (Rawdon and Andrew 1997). The aim of the study was to test the effect of TGF- β 1, a potent cell proliferation inhibitor, on the proportion of β -cells in embryonic chick dorsal pancreatic buds *in vitro*, with short-term exposure to high levels of glucose in Ham's F12.ITS medium. Five-day old chick dorsal pancreatic buds were cultured in serum-free medium for 7 days. Growth factor-reduced Matrigel was used as the extracellular matrix for culturing the explants as it contains reduced levels of growth factors, including TGF- β 1. Ham's F12.ITS with or without TGF- β 1 was used as the medium in which the explants were cultured to test the response of the developing β -cells to TGF- β 1. A group of explants were also cultured in Ham's F12.ITS with high levels of glucose to test the effect of TGF- β 1 on developing β -cells in the presence of glucose. A fourth group of explants were cultured in a high glucose-containing medium without added TGF- β 1. Explants cultured on growth factor-reduced Matrigel with Ham's F12.ITS showed a much higher proportion of β -cells to α -cells compared to explants cultured on growth factor-reduced Matrigel with Ham's F12.ITS and added TGF- β 1. TGF- β 1 decreased the proportion of β -cells to α -cells, as expected (Rawdon and Andrew 1998; Kramer and Alison 2005). However, the addition of high levels of glucose to the medium for short periods of time increased β -cell proportions only in the presence of TGF- β . The study showed that TGF- β 1 decreased the proportions of β -cells in the chick dorsal pancreatic bud. Glucose, however appeared to only partially rescue β -cells in the avian developing pancreas in the presence of TGF- β 1.

De Gasparo M, Milner GR, Norris PD, Milner RDG (1978) Effect of glucose and amino acids on foetal rat pancreatic growth and insulin secretion *in vitro*. *J Endocr* 77:241-248.

Kramer B, Alison B (2005) The effect of reduced TGF- β 1 and high levels of glucose on the development of embryonic insulin cells *in vitro*. *Voyages in Science: Essays by South African Anatomists in Honour of Phillip Tobias's 80th Birthday*. Eds G Strkalj, N Pather, and B Kramer. Content Solutions, Pretoria. pp 261-276.

Rawdon BB, Andrew A (1997) Development of embryonic chick insulin cells in culture: Beneficial effects of serum-free medium, raised nutrients, and biomatrix. *In Vitro Cell and Developmental Biology – Animal* 44:774-784.

Rawdon BB, Andrew A (1998) Effects of tri-iodothyronine (T3), insulin, insulin-like growth factor I (IGF-I) and transforming growth factor beta1 (TGF- β 1) on the proportion of insulin cells in cultured embryonic chick pancreas. *Anatomy and Embryology* 198:245-254.

*Corresponding author
E-mail: anita.marais@gmail.com

The morphology and morphometry of the bony infrastructure used for experimental studies of oral implantology in dogs

N Maru*, V Nimigean, VR Nimigean, MC Rusu, AC Didilescu, D Salavastru

University of Medicine and Pharmacy "Carol Davila", Faculty of Dental Medicine, Bucharest, Romania

Marked qualitative as well as quantitative alterations occur in the alveolar ridge following the loss of teeth. Thus, during the first year following tooth removal, there is a considerable remodeling of the bone tissue. It was reported, however, that despite this pronounced remodeling, the placement of implants in fresh extraction sockets allowed proper clinical healing. The dog mandible is a well used model for implant research both when placed in healed sites or in extraction sockets and defects. The jaw bone is similar to human bone and is of course of intramembraneous origin. A draw back is that the areas used for implant placement most probably are subjected to chewing and biting forces which may have negative influence on the healing.

For the present study we used, according to the locally acting ethical rules, 5 fresh dog specimens from which the maxillae and mandibulae were drawn and serially cut at 10 µm; morphological and morphometrical data were recorded. The results offer the morphometrical background for experimental studies of oral implantology in dogs.

*Corresponding author
E-mail: nicoletamaru@yahoo.com

The inferior lateral attic (the subincudal space): the topography

N Maru*, V Nimigean, MC Rusu, F Pop, E Tomescu

University of Medicine and Pharmacy Carol Davila, Faculty of Dental Medicine, Bucharest, Romania, University of Medicine and Pharmacy Iulius Hatieganu, Cluj Napoca, Romania

Middle Ear Cholesteatoma spreads through anatomical passages that determine the surgical attitude.

The present study was performed in order to evidence and describe two of the most important topographical spaces of the middle ear involved in cholesteatoma spreading: the inferior lateral attic and the subincudal space.

For this study were used 50 temporal bones, obtained in legal conditions at autopsies, from specimens without any known middle ear pathology. Combined, lateral, anterior and superior approaches were used for the anatomical microdissections of those specimens.

The infero-lateral attic (ILA) must be regarded as a passage similar to the tympanic isthmus rather than a distinctive anatomical space. Located externally to the incus, it is limited superior by the lateral incudomalleolar fold (LIF) and the external wall is represented by the lower part of the attical bony wall. The inferior wall of the ILA is made by the posterior part of the posterior malleolar fold (PMF), including at that level the fold of chorda tympani; the anterior part of the PMF separates the Prussak's space to the ILA. The anterior wall of the ILA is represented by the neck of malleus and the ligamentar part of the external malleolar fold. Except the anatomic opening of the ILA below isthmus tympanic posticus into mesotympanum, weak parts of its walls can individually present as additional drainage pathways into the Prussak's space or the lateral malleolar space.

The anatomy and topography of the ILA correlates with the aeration and drainage pathways of the retraction pouches of the tympanic membrane, in the pathogenesis of the middle ear cholesteatoma.

*Corresponding author
E-mail: nicoletamaru@yahoo.com

Standardisation of morphological types of intraparenchymal distribution of the hepatic veins – III. Right hepatic veins

P Matusz*, AM Pusztai, DE Zahoi, E Hordovan

Department of Anatomy, Faculty of Medicine, University of Medicine and Pharmacy "Victor Babes" Timisoara, Romania

The right hepatic vein is the most important vein of liver's efferent pedicle, both due to its size and to the volume of the drained parenchyma. It is situated in the plane of the right portal fissure between the medial and the right lateral division. The most often encountered is the presence of the right hepatic vein as a unique vein. Sometimes, in the plane of the right portal fissure may appear an inferior right hepatic vein and a middle right hepatic vein (usually of smaller sizes). We analyzed and standardized the morphological types of the right hepatic veins on a study material of 150 hepatic corrosion casts. They were made by injecting with plastic (AGO II paste and TECHNOVIT 7143) of the hepatic vasculo-ductal systems, followed by corrosion of the hepatic parenchyma with hydrochloric acid. In standardizing the morphological types of the right hepatic veins we considered three parameters: the general aspect of the venous trunk (long or short), the number of affluents of origin and their length. The superior right hepatic vein, having a constant presence (100%), is the largest collector in the plane of the right portal fissure. Considering both the sizes and the number and position of the affluents of the trunk of the right hepatic vein, as well as the modality of collecting of the right postero-superior vein and of the right transverse vein, there are three morphological types of spatial distribution of the right hepatic vein: Type I (65.33% cases), with a long, well individualized venous trunk, receiving into its distal portion the right antero-lateral vein and the right antero-medial trunk; Type II (24.67% cases), with a short venous trunk, formed by the confluence of the right anterior trunk with the right transverse trunk; Type III (10% cases), with a short venous trunk, formed by the confluence of the right anterior transverse vein with the left transverse vein. The inferior right hepatic vein was found in 10.67% cases. The middle right hepatic vein was found in 4% cases and in all cases where it was present it was the smallest of all. According to the number of the right hepatic veins found, we analyzed the modality of venous segmentation of the right part of the hepatic parenchyma and noticed that: in 89.33% cases there is only a single right hepato-venous segment, in 8% cases there are two right hepato-venous segments (a superior and an inferior one), and in 2.67% cases there are three right hepato-venous segments (superior, middle and inferior), according to the number of right hepatic veins present in the plane of the right portal fissure. Knowing these aspects of venous drainage of hepatic parenchyma could facilitate planning hepatic resection and transplant surgery.

(Supported by CEEX 175/2006).

*Corresponding author
E-mail: matusz@umft.ro

Repeated, brief seizures induce long-lasting rearrangement of ionotropic glutamate receptor subunits in the rat hippocampus

A Mihály^{1*}, E Dobó¹, E Molnár², A Bagosi¹, M Bakos¹, B Szűcs¹, A Vincze¹, N Károly¹

¹Department of Anatomy, University of Szeged, Szeged, Hungary, ²Department of Anatomy, University of Bristol, Bristol, UK

Repeated, brief epileptic seizures were induced with intraperitoneally injected 4-aminopyridine (4-AP) in adult Wistar rats, for two weeks, on a daily basis. The symptoms were observed carefully and evaluated on the Racine's scale. One day after the last injection and seizure, rats were decapitated in deep anesthesia, the brains were frozen in liquid nitrogen, and sectioned in the horizontal plane. Another group of rats were observed for two more weeks, without 4-AP injections, and decapitated as written above. The 15 µm thin sections were blotted onto nitrocellulose membranes, the membranes were fixed and the proteins detected with immunohistochemical method, using alkaline phosphatase-labeled secondary antibodies. The following subunit antibodies were used: NR1, NR2A, NR2B, GluR1, GluR1 flop, GluR2, pan-AMPA (GluR 1-4, recognizing every AMPA subunit), and KA2. The immunostained membranes were scanned, and different layers of the hippocampus and neocortex were analyzed with densitometry. Hippocampi were also stained with a modified Timm's stain, and the stained area has been

analyzed with densitometry, similarly to the immunostained preparations. The learning ability of repeatedly convulsing rats was evaluated with a Morris water-maze test. In the hippocampus, an overall decrease of NR1 subunits was observed. NR2B remained unchanged, but NR2A increased significantly in every layer. GluR1 and GluR2 decreased in most of the areas and layers. The increase of the GluR1flop was observed in most of the layers. KA2 did change in the stratum lucidum of CA3, only. Less pronounced, but significant changes were detected in the entorhinal, perirhinal and somatosensory cortices, where the decrease of the NR1 subunit was observed. The NR2A and NR2B subunits displayed significant increases. The GluR1 and GluR2 subunits decreased only in the entorhinal and perirhinal areas. In the same areas GluR1flop showed a significant increase. Significant changes were detected in the KA2 subunit density: decrease in the entorhinal and perirhinal areas and increase in the somatosensory cortex.

Supported by OTKA T32566, GB-8/2003, OMFB-1921/2002.

*Corresponding author
E-mail: mihaly@anatomy.szote.u-szeged.hu

Origin and immunocytochemical characterization of microglial cells in the avian pineal gland

D Molnar*, CL Frank, B Vigh, I Olah, N Nagy

Department of Human Morphology and Developmental Biology, Faculty of Medicine, Semmelweis University, Budapest, Hungary

The origin of the microglial cells in the central nervous system and in the pineal gland is still a matter of debate. Besides the neuroepithelial origin recently the mesodermal or hemopoietic origin is generally accepted but not experimentally proved. The aim of these studies was to characterize immunocytochemically the microglial cells and to provide experimental evidence for their origin in the pineal gland.

Different cell specific markers have been used for immunocytochemical characterization of the microglial cells; hemopoietic (CD45 and QH1 for chicken and quail cells, respectively); B lymphocyte (Bu1b and Bu1a for chicken and quail cells, respectively); T lymphocyte (CD3, CD4, CD8); macrophage (68.2, 74.2); MHC class II (TAP1, P2M11, 2D5) and avian dendritic cells (74.3, NIC2).

In the pineal parenchyma a poorly and highly ramified CD45+ hemopoietic cells can be distinguished. The former one expressed 68.2 and 74.2 macrophage markers while other was positive for B cell specific antibody (Bu1) and Ricinus communis agglutinin I (RCA I) a lectin specific for avian microglial cells. Recently, we do not know that the poorly and highly ramified cells represent two subpopulations of microglial cells or different maturation stages of the same cell type. The immunocytochemical characterization of the Bu1b+/CD45+/RCA I+ cells strongly suggested their hemopoietic origin and expression of MHC class II antigen makes them capable for antigen presentation.

To clarify the origin of microglial cells chick-quail chimera has been made: quail pineal gland from 10 days old embryo was isolated and transplanted into the coelomic cavity of a 3 days old, host chicken embryo and further incubated for 14 days. Hemopoietic cells from the chick host migrated to and colonized the grafted pineal gland where these host-derived cells differentiated into CD45+/Bu1b+/MHC II+/RCA I+ microglia cells. The presence of two types of cells (poorly and highly ramified) in immunologically matured birds indicates that hemopoietic microglial precursor cells enter the pineal gland not only at early embryonic age but also after hatching –perhaps throughout life time.

*Corresponding author
E-mail: david@ana2.sote.hu

A delay in urinary tract maturation causes vesicoureteral reflux in the *Pax2*^{1Neu+/-} mouse

IJ Murawski^{1,2}, DB Myburgh¹, J Favor³, IR Gupta^{1*}

¹Department of Pediatrics, McGill University Health Center, Montreal, Quebec, Canada, ²Department of Human Genetics McGill University Health Center, Montreal, Quebec, Canada, ³GSF- Institute of Human Genetics, Neuherburg, Germany

Vesicoureteral reflux (VUR) is a congenital urinary tract defect that leads to the retrograde flow of urine to the kidneys. Clinical studies demonstrate that patients with VUR frequently have shorter intravesical ureters, the portion of the ureter within the bladder. This shortened intravesical ureter is likely caused by improper insertion of the ureter within the bladder wall and leads to an incompetent ureterovesical junction. VUR is known to spontaneously disappear in as many as 2/3rds of affected children, indicating that the condition can resolve over time, and supporting a theory that VUR is caused by a delay in urinary tract development. In children in which VUR resolves, it is presumed that the ureter has grown and formed a more competent ureterovesical junction. *Pax2* is a transcription factor critical for kidney development, and when mutated in humans it causes both VUR and kidney malformations in a condition known as Renal-Coloboma Syndrome. The *Pax2*^{1Neu+/-} mouse harbors the same mutation as in affected humans and we demonstrate that 32% of *Pax2*^{1Neu+/-} mice exhibit VUR, providing evidence for a urinary tract defect. At postnatal day 1, we found the length of the intravesical ureter to be significantly shorter in *Pax2*^{1Neu+/-} mice compared to their wildtype littermates, which may predispose them to VUR. To determine if there is an embryonic origin to the development of VUR, we characterized the position of the ureteric bud along the mesonephric duct. During development the ureteric bud grows from the mesonephric duct and develops into both the mature ureter and kidney. At embryonic day (E) 10.5, we found the ureteric bud exits from a more caudal position along the mesonephric duct in *Pax2*^{1Neu+/-} mice compared to wildtype mice. We crossed *Pax2*^{1Neu+/-} mice to *Hoxb7/GFP*^{+/-} mice to examine urinary tract development in detail. Embryos collected between E10 and E17 revealed that *Pax2*^{1Neu+/-} embryos have a delay in the separation of the ureter from the mesonephric duct. This in turn causes a delay in the union of the ureter with the bladder wall. Furthermore, *Pax2*^{1Neu+/-} embryos have intravesical ureters that have lost their oblique angle of entry into the bladder, which may affect the competence of the ureterovesical junction. We are currently examining ureter morphology and musculature in detail. Our results provide the first experimental evidence that vesicoureteral reflux may arise from a delay in urinary tract maturation and an explanation for the clinical observation that VUR can resolve over time.

*Corresponding author
E-mail: guptalab@gmail.com

Origin of the epithelial anlage of the bursa of fabricius

N Nagy^{1*}, AM Goldstein², DJ Roberts³, É Bíró, I Olah¹

¹Department of Human Morphology and Developmental Biology, Faculty of Medicine, Semmelweis University, Budapest, Hungary, ²Department of Pediatric Surgery, Massachusetts General Hospital, Harvard Medical School, Boston, MA, USA, ³Department of Pathology, Massachusetts General Hospital, Harvard Medical School, Boston, MA, USA

The bursa of Fabricius is a central lymphoid organ of birds that is responsible for B lymphocyte development and maturation. It is generally believed that the bursal epithelium is derived from endoderm. However, since the bursa arises from a diverticulum off the cloaca, where endoderm and ectoderm are juxtaposed, both germ layers can contribute to the bursal epithelium. Furthermore, the bursal duct enters the proctodeum, which is an ectodermal derivative of the cloaca, supporting an ectodermal origin for the bursa. The aim of our study was to clarify the endodermal or ectodermal origin of the bursal epithelium. We generated chick-quail tailbud chimeras by transplanting quail tailbud ectoderm into the chicken tailbud and incubating for 12 days. In these chimeric embryos, the developing bursa was comprised of quail ectoderm and chicken hemopoietic cells. The presence of QCPN+/cytokeratin+ bursal epithelium in the grafted quail tailbuds indicated that the bursal epithelial cells were derived from the grafted ectoderm. Using in vitro tissue recombination experiments, followed by intracoelomic transplantation, we found that the bursa mesenchyme did not contain follicles unless the cloacal ectoderm was included. Our findings suggest that the proctodeal ectoderm invaginates into the tailbud mesenchyme to form the epithelium of the bursa.

Supported by grant OTKA T-042558.

*Corresponding author
E-mail: nagyn@ana2.sote.hu

Analysis and standardization of the anastomoses between the affluents of origin of the hepatic veins. Study on corrosion casts

V Niculescu*, P Matusz, AM Pusztai, E Dumitrascu-Doru, B Hogeia

Department of Anatomy, Faculty of Medicine, University of Medicine and Pharmacy "Victor Babes" Timisoara, Romania

The hepatic veins (components of liver's efferent pedicle) are situated in the plane of the portal fissures. The right hepatic vein is situated in the plane of the right portal fissure, the middle hepatic vein in the plane of the main portal fissure and the left hepatic vein in the plane of the umbilical fissure. The presence of anastomoses between the affluents of the hepatic veins is controversial in anatomy, their existence in the normal liver being alternatively accepted or denied. In order to demonstrate the anastomoses between the affluents of origin of the hepatic veins, as well as to discover some of the possible causes of their appearance in the normal liver, we analyzed 100 hepatic corrosion casts (from persons without previous hepatic diseases). The livers were injected with plastic (AGO II paste and TECHNOVIT 7143), followed by parenchyma corrosion with hydrochloric acid. According to the intraparenchymal distribution of the hepatic veins, we considered 3 hepato-venous segments (left, middle and right, the latter having sub segments if there were 1 or 2 supplemental right hepatic veins). Considering the venous trunks connected, the venous anastomoses were classified in 4 size categories (the first order being represented by anastomoses between the trunks of the hepatic veins). According to their location, we found two distinct categories of anastomoses: venous intersegmentary anastomoses and venous intrasegmentary anastomoses. In the 100 hepatic corrosion casts we found 288 anastomoses (the anastomoses of III-rd and IV-th order usually with a diameter larger than 1 mm). In some corrosion casts injected with ultra fluid plastic we found, at the level of liver's inferior margin, numerous anastomoses of superior order but with diameter much less than 1 mm, that were not considered in this study. The 288 anastomoses were classified into 4 size orders, as follows: I-st order – 2.08% (6/288 casts), II-nd order 19.44% (56/288 casts), III-rd order 39.93% (115/288 casts) and IV-th order 38.55% (111/288 casts). The 6 anastomoses of I-st order were always found between the trunks of the right hepatic vein and of the middle hepatic vein (intersegmentary anastomoses). Most of the anastomoses (74.30%, 214/288 casts) were intersegmentary. In 25.70% (74/288 casts) the anastomoses were between the affluents of origin of the same hepatic vein (intrasegmentary anastomoses). The overall analysis of the intraparenchymal distribution of

the venous anastomoses showed 8 morphological types of distribution in the case of the venous intersegmentary anastomoses and 9 morphological types in the case of venous intrasegmentary anastomoses. The situation when the middle hepatic vein and the left hepatic vein form a common trunk of drainage into the inferior vena cava and the right hepatic vein drains alone favors the apparition of intra- and intersegmentary venous anastomoses. These anastomoses appear in the normal liver (without previous hepatic disease). Knowing these aspects of morphologic interrelation between the elements of origin of the hepatic veins could facilitate the planning of surgery for liver resection or transplant, considering that the venous anastomoses interconnect hepato-venous segments.

(Supported by CEEEX 175/2006).

*Corresponding author
E-mail: niculescu.virgil@gmail.com

Aspects regarding the morphological variability of superior thyroid artery

V Niculescu*, P Matusz, A-M Jianu, MC Niculescu, I-C Ciobanu, L-G Stana, E Daescu

Department of Anatomy, Faculty of Medicine, University of Medicine and Pharmacy Victor Babes, Timisoara, Romania

Vascularization of the thyroid gland is realized by two superior thyroid arteries, witch irrigate superior and anterolateral part of thyroid lobe and two inferior thyroid arteries, which irrigate inferior and inferomedial part of the gland. The study was made in the Laboratory of Anatomy at the University of Medicine and Pharmacy Victor Babes, Timisoara, on 120 corpses. To point out superior thyroid artery, we used the method of macroscopic dissection correlated with injection of colored plastic materials (latex). During the dissection we followed the origin, the line, the size and the connections of superior thyroid artery. We come up to the following conclusions: the missing of the superior thyroid artery, unilateral or bilateral, although is written in the anatomical literature. This absence isn't frequent and it exists when the lateral thyroid lobe is missing; the origin of the superior thyroid artery has its variability: 35,8% from the common carotid artery, 36,6% from the external carotid artery, 27,5% from the bifurcation of the carotid artery; the initial direction of the superior thyroid artery may present some variability: ascendant(17%), horizontal (39%) and descendant (44%); in one case we found a common trunk between superior thyroid artery and lingual artery, the origin of the common trunk, in this case, being situated above the carotid bifurcation.

*Corresponding author
E-mail: niculescu.virgil@gmail.com

The incisive canal – an obstacle in oral implantology?

V Nimigean*, VR Nimigean, N Maru, MC Rusu, AC Didilescu, DI Salavastru

The Faculty of Dentistry, University of Medicine and Pharmacy, Bucharest, Romania

To assess whether the incisive canal and its content could represent an anatomic obstacle for implant prosthetic rehabilitation. This study was realised for determination of the accurate implants positioning in the anterior maxilla.

For the evaluation of the typical shape of the incisive canal and surrounding bone with respect to the presence or absence of upper incisors, we accomplished dissections on formolized human cadavers (25) and CT examinations on 15 young adult patients which needed implant prosthetic rehabilitation in the region of maxillary central incisors.

The alveolar bone quantity in the incisor region was significantly reduced in high at the level of the labial surface, the alveolar ridge being in a posterior and palatal position in the edentulous maxillae compared with the dentate ones. It was

quantitatively confirmed that the distance between the alveolar ridge and the incisive foramen decreases and the angle from the horizontal plane of the alveolar bone increases following the loss of the incisors,

Accurate implant placement in the anterior maxilla is essential in achieving optimal prosthetic rehabilitation with proper function and acceptable aesthetic and phonetic demands. Bone resorption together with an enlarged incisive foramen can determinate the incisive foramen penetration through implant osteotomy. The anterior maxilla can be a critical region for the implants placement.

Artzi Z, Nemcosky CE, Bitlitum I, Segal P (2000) Displacement of the incisive foramen in conjunction with implant placement in the anterior maxilla without jeopardizing vitality of nasopalatine nerve and vessels: a novel surgical approach. *Clinical Oral Implants Research* 11(5):505-510.
Cavalcanti MG, Yang J, Ruprecht A, Vannier MW (2004) Accurate linear measurements in the anterior maxilla using orthoradially reformatted spiral computed tomography. *Anat Embryol* 208(4):265-271.
Nimigean V, Maru N, Nimigean VR (2004) Anatomie clinica si topografica a capului si gatului. Ed. Universitara „Carol Davila” – Bucuresti.

*Corresponding author
E-mail: vandanimigean@yahoo.com

Morphological aspects of human oocytes after cryopreservation

SA Nottola¹, M Maione¹, G Coticchio², L De Santis³, G Macchiarelli^{4*}, S Bianchi⁴, S Cecconi⁵, G Scaravelli⁶, A Borini²

¹Department of Anatomy, University La Sapienza, Rome, Italy, ²Tecnobios Procreazione, Bologna, Italy, ³University Vita-Salute, IVF Centre, Milan, Italy, ⁴Department of Experimental Medicine, University of L'Aquila, L'Aquila, Italy, ⁵Department of Biomedical Sciences/Technologies, University of L'Aquila, L'Aquila, Italy, ⁶CNESPS, Istituto Superiore di Sanità, Rome, Italy

Oocyte cryopreservation may represent a valid technique of gamete storage for women in need to preserve their reproductive potential. However, in general, oocyte cryopreservation protocols have not been fully optimized and overall clinical success remains quite low. Morphological studies, especially at ultrastructural level, may provide an important contribution in understanding the frequent failure of oocyte viability after cryopreservation. Thus, in order to evaluating the most common freeze-thawing procedures, we studied the ultrastructural characteristics of human preovulatory oocytes frozen/thawed (F/T) with different protocols.

All the oocytes were obtained from patients undergoing *in-vitro* fertilization (IVF) trials after their informed consent. The oocytes were fixed in glutaraldehyde at sampling and after freeze/thawing performed with cryoprotectants at different concentrations. Fresh human preovulatory oocytes were used as controls. The oocytes were processed for light and transmission electron microscopy (LM and TEM) observations.

By LM, both fresh and F/T oocytes appeared rounded, with an normal cytoplasm and a continuous zona pellucida (ZP). Cytoplasmic vacuolization was detected in some F/T oocytes. By TEM, organelles were uniformly dispersed in the ooplasm of fresh and F/T oocytes. Rounded mitochondria with typical cristae were found often associated with tubules and with small vesicles of smooth endoplasmic reticulum (SER), forming respectively mitochondria-SER aggregates and mitochondria-vesicle complexes. Metaphase II chromosomes were eccentrically located in the ooplasm. First polar body was regularly present in the perivitelline space. Cortical granules (CGs) were always present just beneath the oolemma in all the oocytes. Amount and density of CGs appeared abnormally reduced in F/T samples, irrespective of the type and concentration of cryoprotectant used. This was frequently associated with an increased density of the inner ZP. Finally, the presence of vacuolization from a slight to a moderate extent was confirmed by TEM analysis in the ooplasm of some F/T oocytes.

In conclusion, freeze/thawing procedures may generate fine ultrastructural alterations in specific oocyte cytoplasmic structures, presumably responsible for the reduced developmental potential of cryopreserved oocytes.

(Funds by Italian MIUR and Ministero della Salute 2003-2007).

*Corresponding author
E-mail: guido.macchiarelli@cc.univaq.it

Surface reconstruction in scanning electron microscopy and its application to biological fields

E Oho^{1*}, K Suzuki¹, D Koga², T Ushiki²

¹Department of Information Design, Faculty of Informatics, Kogakuin University, Tokyo, Japan, ²Division of Microscopic Anatomy and Bio-Imaging, Graduate School of Medical and Dental Sciences, Niigata University, Niigata, Japan

Scanning electron microscopy (SEM) has been widely used for three-dimensional (3D) surface imaging of biological samples. However, it is often very difficult to measure quantitatively the 3D relation of surface structures (e.g., height, length and/or diameter measurement). To overcome this difficulty, several techniques for obtaining height information in SEM have been proposed to date. Among them, the multiple-detectors method, focusing method and stereometric technique are considered to have potentials for the general applications of sample measurements. Under these circumstances, we have introduced the fundamental innovation of the multiple-detectors method for SEM, because this has some advantages in measuring samples from the view-point of resolution, processing speed, repeat accuracy, and ease of use. In our system, backscattered electron (BSE) signals- produced from a sample - are detected by multiple detectors. Because the detected signals are related to the surface inclination of the area probed by the scanning beam, the surface topography can be obtained with quantitative information at nanometer-scale resolution.

This type of SEM, or 3D-SEM, has a long history of development (Lebiedzik 1979) and has been produced by some SEM manufacturers according to the requirements of the markets. However, the resolution and accuracy in measurement have been insufficient for general use of this instrument, in comparison with other microscopes such as the scanning probe microscope and confocal microscope. Thus, the purpose of this study is to introduce the intrinsic ability of 3D-SEM in 3D observation

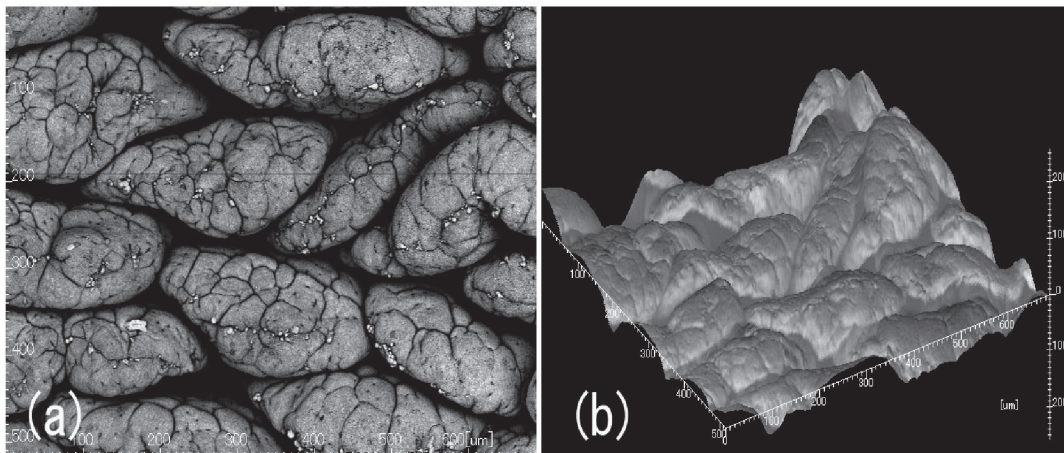


Figure 1A, 1B. A result of 3D observation by our 3D-SEM is shown in the figure below ((a) secondary electron (SE) image, (b) 3D-image obtained through four BSE detectors. Sample: rat intestinal villi). Measurement accuracy increases successfully, because some important improvements have been performed.

and measurement of samples. We also show the usefulness of 3D-SEM for the surface reconstruction of biological samples. Because 3D-SEM is comparatively unconstrained by the sample condition (e.g., size, roughness), focal length, magnification, scanning speed, it has great mobility in 3D-measurement of various samples. The development of reconstruction principle of the surface topography from BSE signals, as well as the quality of acquisition data, is important to improve performance.

Lebiedzik J (1979) An automatic topographical surface reconstruction in the SEM. *Scanning* 2:230-237.

*Corresponding author
E-mail: oho@cc.kogakuin.ac.jp

Hypothalamic arcuate nucleus: neurons in the meeting-point of central autonomic and neuroendocrine regulatory systems

M Palkovits

Neuromorphological and Neuroendocrine Research Laboratory of the Hungarian Academy of Sciences and the Semmelweis University, Budapest, Hungary

The arcuate nucleus, an elongated group of cells in the medio-basal hypothalamus occupy a key position in neuroendocrine and autonomic regulatory mechanisms of the central nervous system. More than 50 years ago, the parvicellular neurosecretion, as a concept has been introduced on the basis of studies by what the secretory activity of arcuate neurons into the pituitary portal vessels had been clearly demonstrated. The nucleus consists of a variety of peptidergic and dopaminergic neurons. The vast majority of these neurons have been coded to express more than one neuropeptides and/or neurotransmitters. Up to date, 11 neuropeptides have been demonstrated in the nuclea that may act, depending of their target sites as neurohormones, neuromodulators or neurotransmitters.

Neurons in the arcuate nucleus receive neuronal and humoral inputs. The neuronal signals can be classified as intranuclear (internal organization of cells for common response to proper stimuli), hypothalamic (mainly from the paraventricular, periventricular and ventromedial nuclei, and from cells in the dorsolateral hypothalamic area) and extrahypothalamic inputs (from the viscerosensory nucleus of the solitary tract and brainstem biogenic amine cell groups). Significant afferent signals arise through the blood circulation, especially through the subependymal plexus of the median eminence which branches terminate in the medial part of the arcuate nucleus. This part of the nucleus (especially the arcuate nucleus/median eminence angle) serves as an “open gate” for humoral signals and certain blood-born substances since this part of the nucleus lacks of blood-brain barrier. Furthermore, the penetration of intraventricularly injected neurotropic virus into the medial portion of the nucleus, as well as the presence of supraependymal nerve terminals in this area all indicate that the “gate” is open for proper inputs arising through the cerebrospinal fluid.

The arcuate neurons have a wide spectrum of efferent targets in the brain, including hypothalamic (paraventricular, periventricular, dorsolateral hypothalamic neurons), brainstem and spinal autonomic cell groups. The known functional role of arcuate neurons includes neurosecretory and dopamine controls of certain neuroendocrine activity, like the control of the expression and release of prolactin, gonadotrops and growth hormone in the pituitary gland. Arcuate neurons are sensitive to various stressors. As a response to acute stress, *c-fos* expression can be demonstrated in the arcuate nucleus within minutes after stimuli. The central role of the arcuate nucleus in the regulation of food intake and the energy homeostasis of the body are demonstrated and discussed in detail. Feeding-related peripheral hormones, like insulin, leptin and ghrelin pass the “arcuate gate” and act on neuropeptide Y (NPY)-, agouti-related peptide (AgRP)-, pro-opiomelanocortin (POMC)- and CART-related peptides-expressing neurons. In addition, signals from the upper gastro-intestinal tract may also reach arcuate neurons *via* vagus - nucleus of the solitary tract – ascending pathways to the hypothalamus. The arcuate neurons transfer the food intake-related signals to the efferent loop of the feeding regulatory neuronal circuit (paraventricular and dorsolateral anorexigenic and orexigenic neurons, respectively). In the arcuate nucleus, the alternating inhibitory interactions of NPY/AgRP *versus* POMC/CART neurons serve as a very sensitive and specific balance in feeding.

E-mail: palkovits@ana.sote.hu

Left thoracic duct in donkey

MR Paryani^{1*}, H Gilanpour²

¹Department of Basic Sciences, Faculty of Veterinary Medicine, Islamic Azad University, Karaj branch, Karaj, Iran, ²Department of Basic Sciences, Faculty of Veterinary Medicine, University of Tehran, Tehran, Iran

Thoracic duct is a duct that drains the lymph from the cisterna chyli into the venous angle of the cranial vena cava. The thoracic duct in the horse is situated on the right side (Getty 1975; Nickle et al. 1981), but in rare cases the thoracic duct has been reported (Nickle et al.1981; Gilanpour et al. 2005).

In this case the course and position of the thoracic duct in donkey seems to be similar to the horse. In this case the thoracic duct originated from the cisterna chyli passed through the aortic hiatus of the diaphragm and enters to the thoracic cavity. It was situated on left of the median plane on the dorsal aspect of aorta. The thoracic duct was totally on the left side in its course. At the level of fifth thoracic vertebra it inclines ventrally to the left of esophagus. Finally it entered in to the origin of the cranial vena cava at the jugular venous angle. Regarding the anatomical similarity of equine it seems that existence of left thoracic duct in donkeys maybe considered as a rare case.

Getty R (1975) Sisson and Grossman's the anatomy of the domestic animals. 5th Edition W.B. Saunders Co. Philadelphia, p. 629.

Gilanpour H and Paryani MR (2005) Anatomical study of thoracic duct in Caspian miniature horse. J Facul Vet Med Univ Tehran 60(3):295-296.

Nickle R, Schummer A, Seifrele E (1981) The circulatory system, the skin, and the cutaneous organs of the domestic Mammels. Verlag Paul Parey, Berlin. Hamburg. Vol.3, pp. 322-323, 330-331, 438.

*Corresponding author

E-mail: mrparyani@yahoo.com

A comparison of the *in vitro* effect on *Bulbine frutescens* and *natalensis* on dermal fibroblasts and epidermal keratinocytes: implications for wound healing

N Pather^{1*}, R van Zyl², A Viljoen³, B Kramer⁴

¹School of Anatomical Sciences, Department of Pharmacology, Faculty of Health Sciences, University of the Witwatersrand, Johannesburg, South Africa, ²School of Therapeutic Sciences, Faculty of Health Sciences, University of the Witwatersrand, Johannesburg, South Africa, ³School of Pharmacy, Tshwane University of Technology, Private Bag, Pretoria, South Africa, ⁴Embryonic Differentiation and Development Research Programme, Faculty of Health Sciences, University of the Witwatersrand, Johannesburg, South Africa

In recent years, there has been a growing interest in natural and traditional medicines for the treatment of wounds. The use of such medicinal plant extracts has arguably been based largely on historical or anecdotal evidence, since there is relatively little scientific data supporting these claims. Attempts to find agents that promote wound-healing and that are affordable, effective and non-toxic have a long history. In South Africa, hundreds of different indigenous plants are used to treat wounds and burns. The merits of relatively few of these have been scientifically evaluated. One plant, indigenous to only southern Africa and widely used as a skin remedy is *Bulbine* of the Asphodelaceae family van Wyk and Gericke (2000). The leaf of this plant are filled with a clear gel similar in appearance and consistency to the *Aloe vera* gel. The gel of several species of *Bulbine* is commonly used by both traditional healers and the local population for the treatment of wounds, burns, rashes, itches, ringworm, cracked lips and herpes, and is applied directly to the skin or used in the form of a warm poultice (Hutchings et al. 1996). This study aimed to investigate the effect of *Bulbine frutescens* and *Bulbine natalensis* on normal human dermal fibroblasts and keratinocytes. – two cell types that are integral to the wound healing process in skin: keratinocytes contribute to wound closure by proliferating and epithelializing the wound area (Xue et al. 2004) while fibroblasts stimulate collagen production resulting in wound contraction.

Both cell lines were cultured under standard conditions using Iscove's Modified Eagles Medium (MEM) for the fibroblasts and Dulbecco's MEM for the keratinocytes. Cells were seeded into 96 well plates and once confluent, were treated with vary-

ing concentrations of the leaf extract of *B. frutescens* and *natalensis*. These cultures were then subjected to MTT, WST-1 and BrdU tests to determine the cytotoxicity and proliferation effect of the extracts. The effect of the extracts on cell migration was tested using the 'scratch assay'. In addition, migration of cells across a score was analysed over a 48 hour period

Cell proliferation was present at all concentrations of *B. frutescens* and *natalensis*. Proliferation in the treated cultures was significantly greater than control cultures at concentrations of 0.1-5 and 100-300 µg/ml for *Bulbine natalensis* and at concentrations of 0.1-10 µg/ml for *Bulbine frutescens*. Both extracts exhibited no cytotoxicity. The average time to close the 'score' was 37, 46 and 48 hours for the *Bulbine natalensis*, *Bulbine frutescens* and the control cultures, respectively.

These findings have important implications for the use of these extracts to treat wound healing. The *in vivo* effect of the extracts has been tested on an animal model and the histology assessed.

Hutchings A (1996) Zulu Medicinal Plants: an Inventory. University of Natal Press, Scottsville.

Van Wyk B-E, Gericke N (2000) People's plants. A guide to useful plants of southern Africa. 1st edition. Briza Publications, Pretoria

Van Wyke B-E, Van Oudsthoorn B Gericke N (2002) Medicinal plants of South Africa, 2nd edition, Briza Publications; Pretoria

Xue M, Thompson P, Kelso I, Jackson C (2004) Activated protein C stimulates proliferation, migration and wound closure, inhibits apoptosis and upregulates MMP-2 activity in cultured human keratinocytes. *Exp Cell Res* 299:110-127.

*Corresponding author

E-mail: Pather@wits.ac.za

Anatomo-histological analysis of the juncturae and their relations to the extensor tendons to the dorsum of the hand

Y Pınar^{1*}, O Bilge¹, F Govsa¹, S Celik¹, H Aktug²

¹Department of Anatomy, Faculty of Medicine, Ege University, Izmir, Turkey, ²Department of Embryology and Histology, Faculty of Medicine, Ege University, Izmir, Turkey

The extensor digitorum communis (EDC) tendons emerge through the fourth dorsal component onto the dorsum of the hand, they are together distally by an oblique interconnections, juncturae tendineum (JT). The JT may play coordination of extension of hand, force redistribution, stabilization of the metacarpophalangeal joint.

The JT were studied for gross appearance, size, shape, thickness, location and distribution with the dorsum of the hand in fifty-four cadavers. The JT were recorded to the adjacent tendons of origin and insertion, the distance from the radiocarpal joint, and by the intermetacarpal (IMC) space. The first IMC space was defined as the space between the metacarpals to the thumb and index fingers, and second, third and fourth spaces were between the index and long, long and ring, ring and small fingers, respectively. Measurements for the morphological different types of JTs were recorded to the nearest 0.01 mm and were statistically analyzed using Student's t test. After standart tissue processing, the sections were embedded in paraffin and cut at 5µ thickness to the JT stained with hematoxylin-eosin and Masson trichrome.

The JT were identified into three groups their anatomo-histological features. The JT type 1 was consisted of filamentous regions within the intertendinous fascia that contained tiny bands of connective tissue. It was found primarily between EDC tendons to the index and middle fingers and between the tendons to the middle and ring fingers. This type of JT was observed present in 57.4% cases in the second IMC, in 16.7% cases in the third IMC and 1.8% cases in the fourth IMC space. The JT type 2 was found thicker than type 1 JT, yet thinner than type 3. This type of JT was detected present in 3.7% cases in the second IMC, 59.3% cases in the third IMC and in 7.4% cases in the fourth IMC space. The JT type 3 is described the longest and thickest of the three types. Type 3 JTs were subclassified into two subtypes as "Y" and "r" depending on their appearance. The type of 3Y was accounted for 14.8% JT in the third IMC space and 53.7% JT in the fourth space. The type of 3r was detected present in 5.55% cases in the third IMC and in 37% cases in the fourth IMC space. In histologic examination, the fibers of Types 1 and 2 JTs were straight. In Type 3 JTs were composed of regularly oriented parallel and crosswise bundles of tendineous tissue.

This study is important in terms of giving accurate knowledge on the anatomo-histological analysis of the JTs and their relations to the extensor tendons to the dorsum of the hand. Difference of histological features of the JT were not described in the classification of previous studies of JTs. An understanding of the structures of the JT and interactions between the

tendons of the fingers is of importance in hand assessment, during reconstructive procedures such as considering tendons for transfer.

- El-Badawi MGY, Butt MM, Al-Zuhair AGH, Fadel RA (1995) Extensor Tendons of the Fingers: Arrangement and Variations-II. *Clin Anat* 8:391-398.
- Hirai Y, Yoshida K, Yamanaka K, Inoue A, Yamaki K, Yoshizuka M (2001) An anatomic study of the extensor tendons of the human hand. *J Hand Surg [Am]* 26(6):1009-15.
- Kitano K, Tada K, Shibata T, Yoshida T (1996) Independent index extension after indicis proprius transfer: excision of juncturae tendinum. *J Hand Surg [Am]* 21(6):992-6.
- Ogura T, Inoue H, Tanabe G (1987) Anatomic and clinical studies of the extensor digitorum brevis manus. *J Hand Surg [Am]* 12(1):100-7.
- Paley D, McMurtry RY, Murray JF (1987) Dorsal dislocation of the ulnar styloid and extensor carpi ulnaris tendon into the distal radioulnar joint: the empty sulcus sign. *J Hand Surg [Am]* 12(6): 1029-32.
- Rockwell WB, Butler PN, Byrne B. (2000) Extensor tendon: Anatomy, injury, and reconstruction. *Plast Reconstr Surg* 106: 1592-1603.
- von Schroeder HP, Botte MJ (1993) The functional significance of the long extensors and juncturae tendinum in finger extension. *J Hand Surg [Am]* 18(4):641-7.
- von Schroeder HP, Botte MJ, Gellman H (1990) Anatomy of the juncturae of the hand. *J Hand Surg* 15A:595-602.
- Tan ST, Smith PJ (1999) Anomalous extensor muscles of the hand: a review. *J Hand Surg [Am]* 24(3):449-55
- Zilber S, Oberlin C (2004) Anatomical variations of the extensor tendons to the finger over the dorsum of the hand: A study of 50 hands and a review of the literature. *Plast Reconstr Surg* 113:214-221.

*Corresponding author
E-mail: yeldapinar@gmail.com

Expression of calcium-binding proteins in the proliferative zones around the cortico-striatal junction of rabbits during pre- and postnatal ages

C Reblet*, A Alejo, T Fuentes, P Pró-Sistiaga, JL Mendizabal-Zubiaga, JL Bueno-Lopez

Department of Neurosciences, School of Medicine and Dentistry, The University of the Basque Country, Leioa (Vizcaya), Spain

Herein we asked whether cells expressing calcium-binding proteins around the cortico-striatal junction are of pallial or subpallial origin. Brains of rabbit embryos between E18-E28 and postnatal P0-P22 were immunoreacted with monoclonal antibodies raised against calretinin, calbindin and parvalbumin. At E18-E21, calbindin- and calretinin-immunoreactive cells were seen in distinct proliferative zones in the vicinity of the cortico-striatal junction. Whereas calbindin-immunoreactive neurons were in the ventricular zone of the ventral pallium (the medial wall of the lateral ventricular angle), calretinin-immunoreactive cells were, nearby, in the subventricular zone of the subpallium at the lateral edge of the lateral ganglionic eminence. From E25 to P22, both, calbindin- and calretinin-immunoreactive cells appeared in the pallial ventricular and subventricular zones around the lateral ventricular angle. Some of these cells resembled migratory neuroblasts. Parvalbumin-immunoreactive cells appeared at P5-P10, albeit they were almost negligible in the proliferative zones around the cortico-striatal junction and the lateral ventricular angle. The results suggest that a number of the calbindin-expressing neurons that are generated in mid-gestation and postnatally are of pallial origin. They also indicate that only a few of the late-generated calretinin-immunoreactive cells may have a pallial source. The origin of the parvalbumin-immunoreactive cells was not ascertained in the present study.

Supported by: UPV/EHU 12090/2000, MYCT 13338/2001, PB 0624-01.

*Corresponding author
E-mail: concha.reblet@ehu.es

The Collection of Clemente Susini's Anatomical wax models at the University of Cagliari

A Riva*, G Conti

Department of Cytomorphology and Museum of Anatomical Waxes, University of Cagliari, Cagliari, Italy

Alike a few European cities, including Budapest, Cagliari houses a collection of anatomical models manufactured in the Florentine Museum of La Specola. The latter that, with the years, became a veritable "Officina di Ceroplastica" (wax modeling workshop), was created in 1780 by Felice Fontana (1730-1805) with the purpose of providing anatomical aids to the teaching of medicine and particularly of surgery, a discipline whose importance had been greatly emphasized following the publication (1761) of the *Sedibus and Causis Morborum*, the capital textbook by Giovanni Battista Morgagni that, by introducing the organ pathology, puts an end to the old holistic-humoral theory of medicine. The waxes of Cagliari, having been produced in Florence between 1803-1805, are later than those of the great collections of the La Specola in Florence and of the Josephinum in Vienna, and represent a work of the maturity of the great Clemente Susini (1754-1814) the chief modeler of the La Specola museum. The dissections reproduced by Susini are the work of Francesco Antonio Boi (1767-1865), the anatomist from the University of Cagliari who had been sent on purpose to Florence (Riva 2007) by the Viceroy of Sardinia Carlo Felice of Savoy (1765-1831). The models which arrived in Cagliari in 1806 are attached to 23 wooden tables that still bear the original tag with Susini's signature and date.

On the basis of the preparations displayed, the 23 showcases can be classified into 6 groups:

- 1 Microscopic and general Anatomy (case I).
- 2 Muscles (cases II; IV; V; VI, VII, VIII, IX, X).
- 3 Vessels and Muscles, with preparation of the left pectoral lymphnodes (case III).
- 4 Somatic -visceral nerves and vessels (cases XI, XII, XIII).
- 5 Sense Organs (cases XIV; XV; XVI, XVII, XVIII).
- 6 Abdominal and Pelvic Viscera (cases XIX, XX, XXI, XXII, XXIII).

No whole human figures are represented. The most complete preparations are those contained in cases III and XII which demonstrate the head and trunk of a female and of a male body, the latter with a detailed representation of the visceral nervous system. A distinctive character of the collection is the relevance given to both visceral and somatic nerves which are accurately shown in more than one third of the models. On the other hand, lymphatics, that are accurately demonstrated in the other collections of Florentine waxes, are shown marginally only in models III and XII. A description of the most interesting anatomical findings present in the models will be given here, particularly in regard to their scientific and didactic usefulness.

Riva A (2007) *Flesh & Wax. the Clemente Susini's anatomical models in the University of Cagliari*. Ilisso: Nuoro, Italy.

*Corresponding author
E-mail: riva@unica.it

Details on the topography and morphology of the lingual nerve at the level of tongue

MC Rusu*, V Nimigean, N Maru, R Cergan, MA Banu, RC Ciuluvica

University of Medicine and Pharmacy Carol Davila Bucharest, Romania

The lingual nerve brings at the level of tongue trigeminal sensory fibers and also sensory fibers of chorda tympani. Conventional anatomical literature deal very little with the lingual nerve morphology and topography at the level of tongue and also there are few references we could find concerning these data. Our aim was to investigate by dissections and microdissections the anatomical features of the lingual nerve at the level of tongue and to correlate our findings with the existing data. For the study we used 5 human adult cadavers bilaterally dissected and also 6 specimens tongue – pharynx – larynx drawn from adult cadavers at autopsy, according to the local acting ethical principles. The lingual nerve (LN) begins giving off its terminal branches at the level of the anterior border of the hyoglossus muscle (HM), when turning around the submandibular duct of Wharton. We encountered 2 morphological types of terminal division of the LN: a) a single primary trunk (50%); b) two primary trunks (50%), one medial, distributed in the middle third of tongue and other lateral, for the anterior third of tongue. No matter the morphological pattern, the terminal branches of the LN were located on the outer surface of the genioglossus muscle (GM), at the inner border of the inferior longitudinal muscle of tongue, forming a nervous layer over the lingual artery (the deep artery of tongue, N.A.). From the primary trunk(s) were leaving 2 groups of branches: a) thin and anastomosed branches for the ipsilateral mucosa of the ventral surface of tongue, configuring a veritable plexus at that level and also distributing at the level of the lateral border of tongue; b) 4 – 9 thick secondary trunks, emerged “in palisade” from the primary trunk(s), with intralingual course that followed the outer surface of the genioglossus muscle towards the dorsal mucosa of the ipsilateral part of tongue, anterior to the circumvallate papillae. That intralingual course of the LN branches is not reflected by any reference we investigated. The distal secondary trunk was sending distinctively a thin branch distributed in the mucosa of the ventral side of the tip of tongue. A specimen presented a branch distally emerged from the left LN that coursed beneath the mucosa of the tip of tongue and distributed in the mucosa of the right border of the tip of tongue. The central tongue carries a paucity of surgically significant lingual nerve fibers. LN-to-LN anastomoses were evidenced and also LN-to-hypoglossal anastomoses were found: a) the loop of the anterior border of the HM was always linking the first emerged branch of the LN to the 12th cranial nerve: to its main trunk, to the styloglossus nerve or to the first or second ascending hyoglossal branches of the 12th nerve; b) anastomoses on the GM. The hyoglossal loops connecting the LN and the hypoglossal nerve may be involved in the lingual – hypoglossal reflex but this must be studied electrophysiologically. In conclusion: (a) anatomical dissection is a reliable method of investigation for the nervous organisation of tongue, at least comparable to more elaborated technique; (b) the lingual nerve terminal branches respect the circumvallate papillae so the sintagm “distributed to the presulcal part of the tongue” must be carefully considered; (c) on the hyoglossus muscle individual patterns of the anastomoses between the lingual and hypoglossal nerves can be recognized; (d) on the genioglossus muscle there are three superposed layers: that of the lingual nerve branches, that of the deep artery of tongue and that of the hypoglossal nerve branches; (e) on the dorsum of tongue the lingual nerves respect a broad longitudinal median area that is rather poorly supplied with consistent nervous branches; (f) to describe the course of the lingual nerve as being “along the lateral border of tongue” it may appear as an undocumented statement; (g) knowledge of the topographical pattern of nerves in the trigeminal tongue serves to avoid iatrogenic injuries and to facilitate surgical procedures at that level.

*Corresponding author
E-mail: anatomon@gmail.com

Collateral circles in neck supplied by the thyroid arteries – a morphological study

MC Rusu^{1*}, V Nimigean¹, N Maru¹, R Cergan¹, MA Banu¹, MC Niculescu²

¹University of Medicine and Pharmacy Carol Davila, Bucharest, Romania, ²University of Medicine and Pharmacy Victor Babes, Timisoara, Romania

Collateral circles in neck own a particular importance in compensating the symptoms due to the unilateral occlusion of the common carotid artery. Also, surgical procedures at the level of the thyroid gland and larynx rise the problem of a good knowledge of the arterial morphology at that levels. The present study was designed to investigate the possible morphologies of the thyroid arteries anastomoses. For the study 20 human adult specimens were dissected, 15 in cadavers and other 5 on laryngeal specimens that were drawn at autopsies. Dissections evidenced bilateral and unilateral anastomoses of the thyroid arteries, that were classified as extralaryngeal and intralaryngeal, the former constantly being represented by the supraisthmic arcade made by the superior thyroid arteries and the retrolobar anastomoses of the superior and inferior thyroid arteries. Constant intralaryngeal anastomoses were those of the superior laryngeal artery with the inferior laryngeal artery and, respectively, with the cricothyroid artery. The analogy with the cardiac collateral circulation, the thyroid arteries anastomoses may be classified as intrathyroid and interthyroid arterial anastomoses. We also present in this paper a rare variant that we didn't find described in the references we investigated, represented by the paramedian perilaryngeal anastomose of the suprahyoid branch emerged from the lingual artery and the cricothyroid artery sent by the superior thyroid artery. The collateral circles in neck are supplied by the thyroid arteries; the clinicians must be aware of their possible functional value and the surgeons must take into account these arterial morphologies while acting on the neck viscera.

*Corresponding author
E-mail: anatomon@gmail.com

Comparison of four methods for the estimation of intracranial volume: a gold standard study

B Sahin^{1*}, N Acer², OF Sonmez³, M Emirzeoglu¹, H Basaloglu⁴, A Uzun¹, S Bilgic¹

¹Department of Anatomy, Medical School, Ondokuz Mayıs University, Samsun, Turkey, ²Allied Health School, University of Mugla, Mugla, Turkey, ³Neurosurgery Clinic, Gazi Governmental Hospital, Samsun, Turkey, ⁴Department of Anatomy, Medical School, Adnan Menderes University, Aydın, Turkey

Investigators can infer how much reduction in volume has occurred since brain volume was at its peak, by combining measures of brain volume with measures of intracranial volume (ICV). Several methodologies have been proposed to assess the ICV. However, we have not seen a gold standard study evaluating the results of the methodologies for the assessment of ICV. In the present study the actual intracranial volume of 20 dry skulls was measured using the water-filling method, using this as a gold standard. Anthropometry, cephalometry, point-counting and planimetry techniques were applied to the same skulls to estimate the ICV. Anthropometric and cephalometric measurements were carried out directly on skulls and roentgenograms, respectively. Consecutive computed tomography sections at a thickness of 10 mm were used to estimate the ICV of the skulls by means of the point-counting and planimetry methods. The mean (\pm SD) of the actual ICV measured by the water-filling method was $1262.0 \pm 160.4 \text{ cm}^3$, ($1389.5 \pm 96.5 \text{ cm}^3$ for males and $1134.5 \pm 94.3 \text{ cm}^3$ for females, respectively). Our results showed that the estimated values obtained by all four methods differed from the actual volumes of the skulls ($p < 0.05$). The data obtained by anthropometry resulted in over-estimation. However, cephalometry, point-counting and planimetry methods produced under-estimation. After calibration, there were no significant differences between the actual volumes and the results of the four methods ($p > 0.05$). While the anthropometric method is easy and quick to apply, its result may deviate from the actual values. The optimized stereological techniques of point-counting and planimetry methods may provide unbiased ICV results since they take the third dimension of the structures into account.

*Corresponding author
E-mail: bsahin@omu.edu.tr

Confocal microscopy for dynamic morphology of living tissue/ cells: with special reference to Ca^{2+} dynamics in peripheral nervous system

Y Satoh*, T Saino, H Akutsu-Yamauchi

Anatomy (Functional Morphology), Iwate Medical University, Morioka, Japan

Adenosine-5'-triphosphate (ATP) extracellularly which is released from neuronal and non-neuronal tissues interacts with cell surface receptors to produce a broad range of physiological responses. The present study addressed the issue of whether the cells of peripheral nerves (e.g. autonomic nerves: the superior cervical ganglia (SCG) and myenteric plexus, somatic nerves: dorsal root ganglion (DRG) and ischiatic nerve), respond to ATP. To this end, we observed the dynamics of the intracellular calcium ion concentration ($[\text{Ca}^{2+}]_i$) of neurons, satellite cells, Schwann cells and perineurium of rat and golden hamster. Real-time confocal laser scanning microscopy (Nikon RCM/Ab) was used for the imaging of $[\text{Ca}^{2+}]_i$ dynamics.

SCG: ATP produced an increase of $[\text{Ca}^{2+}]_i$ in both neurons and satellite cells; initially, ATP elicited $[\text{Ca}^{2+}]_i$ increase in satellite cells, subsequently, a $[\text{Ca}^{2+}]_i$ change in neurons was observed. P1 purinoceptor agonists had no effect on this process, but P2 purinoceptor agonists induced $[\text{Ca}^{2+}]_i$ increase and suramin totally inhibited ATP-induced $[\text{Ca}^{2+}]_i$ dynamics in both neurons and satellite cells. Ca^{2+} response of neurons occurred at first in cytosol, and then Ca^{2+} wave propagated into nuclei. In satellite cells, Ca^{2+} channel blockers and the removal of extracellular Ca^{2+} , but not thapsigargin-pretreatment, abolished ATP-induced $[\text{Ca}^{2+}]_i$ dynamics. In contrast, thapsigargin-pretreatment abolished ATP-induced $[\text{Ca}^{2+}]_i$ dynamics in neurons. Reactive blue-2 (P2Y antagonist) inhibited the ATP-induced reaction on neurons alone. Uridine-5'-triphosphate (UTP; P2Y agonist) caused a $[\text{Ca}^{2+}]_i$ increase in neurons and α, β -methylene ATP (P2X agonist) caused a $[\text{Ca}^{2+}]_i$ increase in satellite cells. We concluded that neurons of SCG respond to extracellular ATP mainly via P2Y purinoceptors and that satellite cells respond via P2X purinoceptors.

Myenteric plexus: We determined that ATP induced $[\text{Ca}^{2+}]_i$ increase in enteroglia, and only a part of enteric neurons responded to ATP. However, the subtype of purinoceptors could not be examined, because ATP-induced muscle contractions moved the specimens, therefore it was hard to apply different stimulants.

Dorsal root ganglion: In contrast to SCG, DRG neurons showed morphological heterogeneity. In accordance with it, Ca^{2+} response of DRG was not uniform. Generally, satellite cells covering small neurons often respond to ATP, ATP could stimulate the satellite cells of large neurons in a few cases. UTP elicited responses of some satellite cells. Only a part of neurons showed $[\text{Ca}^{2+}]_i$ increase via purinoceptors. The heterogeneity on ATP-induced Ca^{2+} signaling of DRG was incredible.

Ischiatic nerve bundle: Injuries of peripheral tissue stimulate nerves. Peripheral nerves are surrounded by perineurium, therefore the response of perineurium may be a first event of nerve stimulation at tissue injuries. ATP induced a $[\text{Ca}^{2+}]_i$ increase of perineurial cells and naked Schwann cells. If perineurium was intact and the Schwann cells were under the perineurial sheet, extra-nerve ATP could not elicit Ca^{2+} response of Schwann cells. Ca^{2+} channel blockers and removing of extracellular Ca^{2+} , but not thapsigargin-pretreatment, abolished ATP-induced $[\text{Ca}^{2+}]_i$ dynamics. This indicated that the $[\text{Ca}^{2+}]_i$ increase was due to an influx of extracellular Ca^{2+} . ATP also elicited an increase of $[\text{Ca}^{2+}]_i$, but P1 receptor agonists had few effects on $[\text{Ca}^{2+}]_i$ dynamics. Suramin (P2 antagonist) totally inhibited ATP-induced $[\text{Ca}^{2+}]_i$ dynamics, but reactive blue 2 did not. UTP induced no significant change in $[\text{Ca}^{2+}]_i$, but α, β -methylene ATP caused a $[\text{Ca}^{2+}]_i$ increase. In conclusion, perineurial cells respond to extracellular ATP mainly via P2X receptors.

Conclusion: ATP can modulate the functions of non-excitatory components of peripheral nerves (e.g. Satellite cells, Schwann cells, enteroglia and perineurium) via P2 receptors. The subtype of purinoceptors may considerably differ in each tissue.

*Corresponding author
E-mail: yisatoh@iwate-med.ac.jp

Chronobiological potential of skin structural transformations: specific aspect of study

NA Slesarenko¹, RF Kapustin^{2*}

¹Department of Animal Anatomy, Moscow State Academy of Veterinary Medicine and Biotechnology named after K.I. Skryabin, Moscow, Russia, ²Department of Animal Morphology, Belgorod State Agricultural Academy, Maiskii Belgorodskoi oblasti, Russia

In the course of conducted investigations, it has been revealed that skin cover of young (under 1 year) foxes, keeping in conditions of industrial complex and being in optimum conditions of life activity, by index of resiliency module surpasses the same foxes from natural biocenoses. Relative lengthening and durability limit when straining are much higher at foxes from natural populations than at animals, being in conditions of limited biodynamics. Environmental conditions influence greatly on structural forming of skin by reaching 3-years age, and it is accompanied by perceptible deterioration of its biomechanical potencies at mature foxes of cage keeping regime. The increase of such indices as durability limit when straining and resiliency module has been observed at the same time at the same foxes from natural populations with deterioration of parameters of relative skin lengthening. Thus, skin cover of mature foxes from natural populations by its biomechanical characteristics surpasses the same at foxes, keeping in conditions of prolonged hypokinetics. Young (under 1 year) wild minks excel their analogues, keeping in a cage, in an index of relative lengthening and yield in figures expressions of resiliency module, while the differences in durability limit when straining aren't found. In later age periods (3 years and older) representatives of natural biocenoses show high indexes of relative lengthening and essential deterioration of resiliency module and durability limit when straining as compared with minks in a cage. Therefore, skin cover of wild minks surpasses skin cover of cage animals in elastic – deformable characteristics. It has been noticed during study of age dynamics of biomechanical indexes of skin cover, that natural increase of indexes of relative lengthening and durability limit when straining under 3-years age is observed at cage foxes and their further deterioration according to age, while resiliency module decreases with age naturally. Representatives of natural biocenoses demonstrate analogous picture on alteration of relative lengthening and coinciding with it dynamics of resiliency module, while durability limit when straining increases with age naturally. Deformable indexes of cage minks reduce with age, but durability characteristics increase. Representatives of wild fauna show decrease of relative lengthening and durability limit when straining and simultaneous increase of resiliency module. At the same time, morph – metric research of the material hasn't revealed correlation of biomechanical parameters of skin with such indexes as the whole total thickness of derma and relative representation of its layers, although young cage foxes and minks surpass their wild coevals in intensity of growing process and it requires elaboration of complex chronobiological approach for revealing more compact system of informative signs and examination of their distribution in area.

*Corresponding author
E-mail: romankapustin@mail.ru

“Melakril” preparation influence on trade characteristics and dermal integument of mink (*Mustela*)

NA Slesarenko¹, VG Ostankov¹, RF Kapustin^{2*}

¹Department of Animal Anatomy, Moscow State Academy of Veterinary Medicine and Biotechnology named after K.I. Skryabin, Moscow, Russia ²Department of Animal Morphology, Belgorod State Agricultural Academy, Maiskii Belgorodskoi oblasti, Russia

“Melakril” implantation realizes progressive morphogenesis of dermal integument, as biodermal system and rises trustworthy improvement strength and elastic-dermatation characteristics of dermal tissues. On its trade-technological indices, structural appearance and metabolic activity, the dermal integument of minks, implanted by hormonal preparation “Melakril” often excel its control analogues. The thickness of epidermis of implanted animals yields to tested ones, and that connected correlate with rising of thick-haired integument. Hide tissue of one year old age animals is characterized by denser in comparison with control one, by package of collagen fiber, but less quantity of representation of elastic component. Implantation of preparation to young minks is accompanied by rising of refraction degree of collagen and of activity its trophic and consolidation functions. Hair follicles in dermal integument of animals of tested group lie less deep ($612,3 \pm 31,3$ mkm) than at control one ($704,0 \pm 20,8$ mkm), and it prevents appearance the defect as “draught” in dressed hide of tested group rising of firm fur articles. Implantation of hormone preparation “Melakril” doesn’t influence of length, thickness, and softness of hair, but it promotes to rising its density and thickness of hair integument on 7,1 thousand unites / sm^2 , as well as on 1,2% of its specific weight, that improves the quality of hides. The preparation “Melakril” doesn’t provoke changes in chemical composition of hides of tested animals. The use of preparation “Melakril” in fur farming industry differs by high economy expediency.

*Corresponding author
E-mail: romankapustin@mail.ru

Ultrastructural features of common sperm defects in the cane rat (*Thryonomys swinderianus*)

JT Soley^{1*}, HJ Els²

¹Department of Anatomy and Physiology, Faculty of Veterinary Science, University of Pretoria, South Africa, ²Electron Microscopy Unit, Faculty of Veterinary Science, University of Pretoria, South Africa

The cane rat or grasscutter is widely distributed throughout sub-Saharan Africa and its potential for alleviating the continent’s chronic protein shortage has been recognized. However, little is known about the reproductive biology of this rodent. In view of the fact that the identification of sperm abnormalities forms an important aspect of semen evaluation, this paper describes the principal sperm defects observed in cane rat semen.

Semen was collected from the ductus deferens of six healthy and sexually mature male cane rats slaughtered at the Irene Animal Production Institute, Gauteng, South Africa. The samples were fixed in 3% glutaraldehyde in 0.1 M sodium cacodylate buffer, post-fixed in similarly buffered 1% osmium tetroxide and routinely prepared for scanning (SEM) and transmission (TEM) electron microscopy.

The most obvious head defects observed were vacuolar defects, bizarre heads and variations in head shape and size. On SEM, the vacuolar defect manifested as a variable number of crater-like depressions on the surface of the sperm head. The craters were generally restricted to a band immediately beneath the caudal termination of the acrosome forming the typical “diadem” defect. On TEM the craters were seen to be confined to the nucleus and communicated with the peri-nuclear space via a narrow stalk. They did not open onto the cell surface but were covered by the acrosome or post-acrosomal dense lamina. Bizarre heads took on a number of forms but characteristically were large cells with misshapen nuclei. Cane rat sperm displayed a wide variation in head shape and size. This pleomorphism made it difficult to accurately assess this anomaly. However, heads with a narrow base (pyriform/tapered heads) and those with a broad base (often associated with abaxial tail

implantation) were obvious and commonly encountered. Apart from a few instances of acrosome lipping, no acrosome defects were observed in the material studied.

The principal tail defects were double tails, stump tails, kinked tails and bent tails. SEM of double-tailed sperm generally revealed a normal head and two perfectly formed tails consisting of a midpiece, chief-piece and end-piece. Separation of the two tails was variable along the length of the double flagellum. The morphology and alignment of the axoneme, mitochondrial sheath and connecting piece of the neck region all appeared normal when viewed by TEM. Stump tails displayed a variety of forms and were best visualized by SEM. In some instances the tail was rudimentary, consisting only of a small bead of cytoplasm attached to the base of the head. In other cells the tail was of variable but shortened length and generally displayed no obvious regional characteristics. Kinked tails generally appeared normal except that the head and tail were oriented at right angles to each. Tail bending most often occurred in the region of the midpiece where it was sharply reflected and often associated with a cytoplasmic droplet. Tail coiling, typical of the "Dag defect" was only occasionally seen in the material examined.

Multiple defects were common in cane rat sperm. Nuclear vacuolation (the diadem defect), for example, was often associated with double-tailed sperm as well as with stump-tailed sperm.

The sperm defects observed in cane rat sperm have also been described in various other mammalian species. Nuclear invaginations (vacuolation) have specifically been identified in elongating spermatids and epididymal sperm in two other hystricomorph rodents and this defect would appear to be particularly common to this group of animals. Although no causative factors could be determined for the presence of the various defects in the animals studied, the fact that a number of the defects have been associated with infertility/subfertility makes it important to consider these defects when evaluating cane rat semen.

*Corresponding author
E-mail: john.soley@up.ac.za

Application of variable pressure scanning electron microscopy (VP-SEM) to non-coated biological samples: Improvement of the image quality by using helium gas in a low-voltage, low-vacuum environment

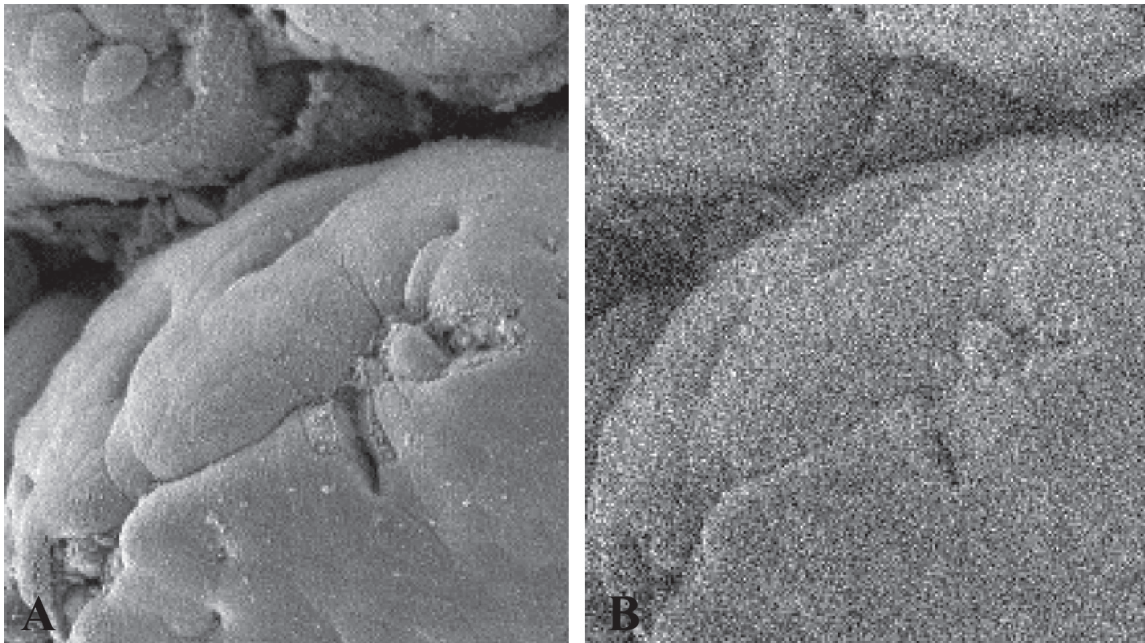
K Suzuki¹, S Yamazaki¹, T Ushiki², E Oho^{1*}

¹Department of Information Design, Faculty of Informatics, Kogakuin University, Tokyo, Japan; ²Division of Microscopic Anatomy and Bio-Imaging, Graduate School of Medical and Dental Sciences, Niigata University, Niigata, Japan

The variable pressure scanning electron microscope (VP-SEM) has been applied to the observation of biological samples without metal coating. It is also helpful for the observation of wet and/or oily samples. The VP-SEM further has the potential to observe a variety of specimens without the need of conventional specimen preparation. However, the range of the proper observation condition (*i.e.*, the relation between the accelerating voltage and pressure) is generally rather narrow in each sample.

We recently showed that the quality of the VP-SEM image signals (by backscattered electrons) is dramatically improved by introducing helium gas into the specimen chamber (Oho et al. 2000). This method is especially useful in low-voltage as well as in a variety of SEM operating conditions, because helium gas can relatively keep the amount of unscattered primary electrons. In the present study, we mainly describe the quality improvement of the image signals obtained from the newly developed environmental secondary electron detector (ESED), which was originally introduced for low-vacuum SEM (Danilatos 1990; Farley and Shah 1991).

Figures 1a and 1b are ESED images operated under air and helium gas, respectively. The accelerating voltage is 5kV, the working distance 14.6 mm, and the pressure 80 Pa for air and 330 Pa for helium. SEM imaging using the ESED under helium gas was helpful in a whole range of pressure. In contrast, imaging in air was practical only under a relatively low pressure. Under the pressure of 330 Pa, no clear image was obtained under air. Surprisingly, it was very difficult to observe the surface structure of samples even under the pressure of 80 Pa (b), which is a common pressure frequently employed in the VP-SEM routine work.



One of the problems for the practical use of helium gas in the SEM is that the charge neutralization effect is reduced to a certain extent in exchange for the increase of unscattered electrons. However, a high pressure condition increases the charge neutralization effect, which may cancel the charging problem. As described above, the VP-SEM is useful for the observation of wet and/or oily samples without the need of conventional specimen preparation. In general, as the pressure of the specimen chamber increases, a wet sample keeps its natural shape. However, the water content of the specimen under the helium gas is unknown. It is necessary to investigate the effective condition of helium gas for achieving practical charge neutralization effect and for retaining a certain amount of water in specimen as well as for obtaining high quality SEM images.

Danilatos GD (1990) The theory of gaseous detector device in the environmental microscopes. *Advances in Electronics and Electron Physics* (ed. by PW Hawkes), Vol.78: pp.1-102 (Academic Press, New York).

Farley, Shah (1991) High pressure SEM of insulating materials---a new approach. *J Microsc* 164:107-126.

Oho E, Asai N, Itoh S (2000) Image-quality improvement using helium gas in low-voltage variable pressure scanning electron microscopy. *J.Electron Microscopy* 49:810-812.

*Corresponding author
E-mail: oho@cc.kogakuin.ac.jp

Morphological approaches in colour vision studies

Á Szél*, P Röhlich, G Halász, Á Berta, A Szabó, Á Lukáts

Department of Human Morphology and Developmental Biology, Semmelweis University, Budapest, Hungary

Colour discrimination in the retina of non-primate mammals is served by two cone types, carrying middle-wave (green, M) and short-wave (blue or ultra-violet, S) sensitive visual pigments, respectively. The two pigments are markedly different from one another, providing a means of immunocytochemical discrimination.

An unexpected topographic separation of M and S cones was found in some rodents. Whereas the dorsal retina is populated by both cone types in the characteristic 10:1 ratio, the ventral retinal half presents an unusual territory in that its exclusive cones are of the short-wave sensitive type. This means that although the global cone density is roughly uniform all over the retina, the two cone types occupy opposite retinal halves. Later, other mammals, among them the rabbit and the guinea pig also proved to be heterogeneous with respect to the distribution pattern of cones. When present, the blue-field always occupies the ventralmost area of the retina. The ventral, short-wave sensitive half continuously scanning the sky for predators might be an advantageous feature. Likewise, the dorsal M-cone-rich retina might be useful for better viewing the green vegetation. Besides, large number of cones express both visual pigments at the same time either within a band or across the entire blue field. The coexistence of two visual pigments within the very same cone cell was also found in other species.

Interestingly, a transitory visual pigment coexpression was also found during the first three weeks of age in rodents. In these animals it is the blue cones that appear first with a dramatic overproduction - as compared to the later expressing green cones. The dominance of the green cones is regained only after the blue pigment is removed from the dual cones. The spatial and temporal coexpression leads to the hypothesis that these elements develop from one another. Transdifferentiation may be the most suitable means to provide for a controllable distribution of the color cones across the retina. There must be a default pathway favouring the differentiation towards the synthesis of the short-wave pigment. The topographical determination of a developmental wave along the dorsal-ventral axis is supported by large numbers of studies that report on the characteristic distribution of proteins in the embryonic eye and dorsal-ventral expression patterns of exogenous opsin genes.

An important question is whether this spatial distribution and temporal sequence can be experimentally modified. Retinal transplants showed relatively normal organotypic maturation, however the paucity of M cones as compared to S cones was a consistent feature. The results of the transplantation experiments indicate that the absence of age-specific environment selectively influences the normal differentiation of M cones, even when the species- and organ-specific factors are available in the host retina.

Omitting the organ-specific environment, similarly to transplants, explanted retinas were completely devoid of M cones. The manipulation coincides with events that are crucial for the differentiation of the green cones. The question addresses recently the identifications of the factors that modify the spatial and temporal distribution of color cones in mammals.

Grants that supported the work: Hungarian OTKA grants: #T-029048 and #T-042524, ETT grant #018/2006.

*Corresponding author
E-mail: szel@ana2.sote.hu

Interrelationship between caveolin-1 and e-NOS: a new perspective

S Tengattini, F Bonomini*, A Fabiano, R Bianchi, R Rezzani

1. Division of Human Anatomy, Department of Biomedical Sciences and Biotechnologies, University of Brescia, Italy

The original intent of the word caveolae is to describe membrane invaginations at the cell surface. Caveolae are rich in glycosphingolipids, cholesterol and structural proteins essential for their formation (Caveolin-1, -2, -3; Anderson 1998; Govers et al. 2001).

It has been shown that endothelial nitric oxide synthase (eNOS) is located in plasmalemmal caveolae and that it directly interacts with the structural proteins of caveolae (in particular with caveolin-1; Feron et al. 2006). This binding determines a negative regulation of eNOS activity and so a decrease of nitric oxide production (Zulli et al. 2006).

Cyclosporine A (CsA), an immunosuppressive drug, decreases cholesterol content in caveolae (disrupting a cholesterol-caveolin complex) and displaces eNOS from caveolae (Lungu et al. 2004).

The aim of this study was to determine if eNOS regulation can play a role in CsA-induced nephrotoxicity, using also a nitric oxide synthase (NOS) inhibitor, L-NAME.

For this work we used caveolin-1 knock-out mice (*cav-1*^{-/-}) and wildtype (*cav-1*^{+/+}).

Both *cav-1*^{-/-} and *cav-1*^{+/+} mice have been divided in eight groups. The animals were injected with CsA subcutaneously and with L-NAME intravenously. The first four groups treated with CsA (15mg/kg/day) for different times, 10 (group 1), 14 (group 2), 18 (group 3), and 22 (group 4) days. The last four groups treated with CsA (15mg/kg/day) and L-NAME (30 mg/kg/day) at the same times of the previous four groups (10, 14, 18 and 22 days).

We evaluated kidney morphology by standard staining, e-NOS expression by immunohistochemical method and p-eNOS (ser1177) expression by immunoblotting. Our results showed that in the *cav-1*^{-/-} mice CsA doesn't alter the renal morphology instead in the *cav-1*^{+/+} and in CsA+L-NAME knock-out and wildtype mice we found alterations like to those found in CsA treated mice. Regarding eNOS expression it is upregulated by CsA treatment in *cav-1*^{-/-} mice compared to all the other groups. Immunoblotting analysis showed that p-eNOS is more expressed in *cav-1*^{-/-} mice treated only with CsA.

Our results show that the nephrotoxic effect of CsA is caveolae-mediated and that eNOS up-regulation is responsible of protection against CsA-induced nephrotoxicity in caveolin-1 knock-out mice.

Anderson R (1998) The caveolae membrane system. *Annu Rev Biochem* 67:199-225.

Govers R, Rabelink TJ (2001) Cellular regulation of endothelial nitric oxide synthase. *Am J Physiol Renal Physiol* 280:F193-F206.

Feron O, Balligand J (2006) Caveolins and the regulation of endothelial nitric oxide synthase in the heart. *Cardiovasc Res* 69:788-797.

Zulli A, Buxton BF, Black MJ, Ming Z, Cameron A, Hare DL (2006) The immunoquantification of caveolin-1 and eNOS in human and rabbit diseased blood vessel. *J Histochem Cytochem* 54:151-159.

Lungu AO, Jin ZG, Yamawaki H, Tanimoto T, Wong C, Berk BC (2004) Cyclosporin A inhibits flow-mediated activation of endothelial nitric-oxide synthase by altering cholesterol content in caveolae. *J Biol Chem* 279: 48794-48800.

*Corresponding author

E-mail: bonomini@med.unibs.it

Roles of autophagy in pathogenesis of lysosome storage disease and neuron death after hypoxic-ischemic brain injury

Y Uchiyama

Department of Cell Biology and Neuroscience, Osaka University Graduate School of Medicine, Osaka, Japan

We have shown that autophagy contributes to the accumulation of vacuolar structures in neurons obtained from CD-/- and CB-/-CL-/- mice, murine models for neuronal ceroid lipofuscinoses (NCLs). In these mutant mice, abnormal vacuolar structures accumulating in neurons of the brains resemble autophagosomes/autolysosomes (Koike et al. 2000; Nakanishi et al. 2001; Koike et al. 2003; Koike et al. 2005). An increased conversion of the molecular form of LC3 was demonstrated for autophagosome formation, from LC3-I, a cytosolic form, to LC3-II. The membrane-bound LC3-II form predominated in both cathepsin D-deficient and cathepsins B and L-deficient mouse brains, while LC3 signals accumulated in granular structures located in neuronal perikarya and axons of these mutant brains and were localized to the membranes of autophagosomes, evidenced by immunofluorescence microscopy and freeze-fracture-replica immunoelectron microscopy (Koike et al. 2005). Moreover, like cathepsin D-deficient neurons, autofluorescence and subunit c of mitochondrial ATP synthase accumulated in cathepsins B and L-deficient neurons, indicating that not only cathepsin D-deficient but also cathepsins B and L-deficient mice could be animal models for neuronal ceroid-lipofuscinosis/Batten disease (Koike et al. 2005). These data strongly argue for a major involvement of autophagy in the pathogenesis of Batten disease/lysosomal storage disorders. Until recently, it remains largely unknown what signaling is essential for autophagosome formation. Interestingly, in the conditional Atg7-knock-out mice where autophagy is absent specifically in the liver or brain, numerous ubiquitinated aggregates are detected in the cytosol of hepatocytes, suggesting that protein ubiquitination may serve as a signal to the autophagic process (Komatsu et al. 2005; 2006). We therefore examined the immunohisto/cytochemical localization of ubiquitin and LC3, and found that in our NCL model mice, positive signals for ubiquitin and LC3 were co-localized on the membranes of granular structures in the neuronal perikarya. From these results it is likely that protein ubiquitination may be involved in signaling for autophagosome formation in NCLs. It has been shown that the lysosomal system including autophagy is activated in the CA1 pyramidal neurons of gerbil hippocampus after brief forebrain ischemia (Nitatori et al. 1995). The mechanism underlying neuronal death in hypoxia and ischemia brain injury is excitotoxicity, while the cell death mode associated with ischemic brain injury still remains controversial. We examined neuron death in the CA1 pyramidal layer of the hippocampus in young mice after hypoxic-ischemic (H-I) brain injury and found that the activation of caspase-3 occurred within 24 hr after H-I injury, while TUNEL-positive neurons appearing abundantly at 3 days after H-I insult were negative for caspase-3 but positive for LC3. These lines of data indicate that autophagy may play an important role in neuron death in the CA1 region after H-I brain injury. Thus autophagy that plays an essential role in the metabolism of mammalian cells is largely associated with pathogenesis of neurodegenerative diseases.

- Koike M, Nakanishi H, Saftig P, Ezaki J, Isahara K, Ohsawa Y, Schulz-Schaeffer W, Watanabe T, Waguri W, Kametaka S, Shibata M, Yamamoto K, Kominami E, Peters C, Figura K, Uchiyama Y (2000) Cathepsin D deficiency induces lysosomal storage with ceroid lipofuscin in mouse CNS neurons. *J Neurosci* 20:6898-6906.
- Koike M, Shibata M, Ohsawa Y, Nakanishi H, Koga T, Kametaka S, Waguri S, Momoi T, Kominami E, Peters C, Figura K von, Saftig S, Uchiyama Y (2003) Involvement of two different cell death pathways in retinal atrophy of cathepsin D-deficient mice. *Mol Cell Neurosci* 22:146-161.
- Koike M, Shibata M, Waguri S, Yoshimura K, Tanida I, Kominami E, Gotow G, Peters C, Figura K, Mizushima N, Saftig P, Uchiyama Y (2005) Participation of autophagy in storage of lysosomes in neurons from mouse models of neuronal ceroid-lipofuscinoses (Batten disease). *Am J Pathol* 167:1713-1728.
- Komatsu M, Waguri S, Ueno T, Iwata J, Murata S, Tanida I, Ezaki J, Mizushima N, Ohsumi Y, Uchiyama Y, Kominami E, Tanaka K, Chiba T (2005) Impairment of starvation-induced and constitutive autophagy in Atg7-deficient mice. *J Cell Biol* 169:425-434.
- Komatsu M, Waguri S, Chiba T, Murata S, Iwata J, Tanida I, Ueno T, Koike M, Uchiyama Y, Kominami E, Tanaka K (2006) Loss of autophagy in the central nervous system causes neurodegeneration in mice. *Nature* 441:880-884.
- Nakanishi H, Zang J, Koike M, Nishioku T, Okamoto Y, Kominami E, Figura K, Peters C, Yamamoto K, Saftig P, Uchiyama Y (2001) Involvement of nitric oxide released from microglia-macrophages in pathological changes of cathepsin D-deficient mice. *J Neurosci* 21:7526-7533.
- Nitatori T, Sato N, Shibana K, Waguri S, Karasawa Y, Araki H, Kominami E, Uchiyama Y (1995) Delayed neuronal death in the CA1 pyramidal cell layer of the gerbil hippocampus following transient ischemia is apoptosis. *J Neurosci* 15:1001-1011.

E-mail: y-uchi@anat1.med.osaka-u.ac.jp

Scanning probe microscopy for imaging human chromosomes

T Ushiki*, O Hoshi

Division of Microscopic Anatomy and Bio-Imaging, Graduate School of Medical and Dental Sciences, Niigata University, Niigata, Japan

Various kinds of microscope using a probing tip have been introduced since the scanning tunneling microscope was invented in 1981, and form a new family of the scanning probe microscope (SPM). The atomic force microscope (AFM), one such SPM, has the advantage in creating topographic images of the sample surface at high spatial resolution in various (vacuum, air and liquid) environments. Thus, the AFM has been applied to the studies of biological samples from DNA to living cells (Ushiki 2003). In this paper, we focused on our AFM studies on the high-ordered structure of human metaphase chromosomes.

We first obtained AFM images of dried chromosomes in the ambient condition (Ushiki et al. 2002). The chromosomes - harvested from human lymphocytes by a standard procedure - were fixed with methanol-acetic acid, treated with 1% tannic acid solution and 1% OsO₄, critical point-dried in liquid CO₂, and observed using a dynamic mode (*i.e.*, intermittent contact mode) in the atmosphere. The morphology of the chromosomes prepared with this technique was well preserved; they were composed of the highly condensed chromatids of a mitotic pair, each of which was characterized by the presence of alternating ridges and grooves. At high magnification, they are composed of tightly packed chromatin fibers about 50-60 nm thick.

We then obtained AFM images of wet fixed chromosomes in a liquid environment (Hoshi et al. 2004); chromosomes prepared by the same method as above were observed using a dynamic mode in a phosphate-buffered saline (PBS) solution. For AFM imaging in liquid, the interaction force between the tip and sample was carefully adjusted to the minimum degree, otherwise chromosomes were easily deformed during scanning, because of their extreme softness in liquid environments. The surface of chromatids in these wet chromosomes was characterized by the presence of alternating ridges and grooves, as observed in the dried chromosomes.

In order to study the structure of chromosomes in the condition much closer to the physiological state, we further obtained AFM images of unfixed, or native, chromosomes in a liquid environment (Hoshi et al. 2006). The three-dimensional surface structure of the isolated chromosomes without any chemical fixation was observed at high resolution using a dynamic mode in an isolation buffer solution. The obtained features were almost the same as those found in the critical point-dried chromosomes as well as the wet fixed samples.

These features indicate that the structure of the chromosome arm is not uniform but heterogeneous because of the presence of highly condensed and less condensed regions in the chromosome.

Hoshi O, Owen R, Miles M, Ushiki T (2004) Imaging of human metaphase chromosomes by atomic force microscopy in liquid. *Cytogenet Genome Res* 107:28-31.

Hoshi O, Shigeno M, Ushiki T (2006) Atomic force microscopy of native human metaphase chromosomes in a liquid. *Arch Histol Cytol* 69:73-78.

Ushiki T (2003) Atomic force microscopy for imaging living organisms: from DNA to cell motion. In: Fujita F ed., *Micromachines as tools for nanotechnology*. Springer, Berlin, pp. 121-130.

Ushiki T, Hoshi O, Iwai K, Kimura E, Shigeno M (2002) The structure of human metaphase chromosomes: its histological perspective and new horizons by atomic force microscopy. *Arch Histol Cytol* 65:377-390.

*Corresponding author

E-mail: t-ushiki@med.niigata-u.ac.jp

The expression of erythropoietin and its receptor in the developing rat retina

D Végvári^{1*}, A Szabó¹, G Deák², Á Lukáts¹, V Doma¹, Ál Berta¹, Á Szél¹

¹Department of Human Morphology and Developmental Biology, Semmelweis University, Budapest, Hungary,

²Eye Clinic, Semmelweis University, Budapest, Hungary

Evidence from a number of studies indicates that the erythropoietin (EPO) does not only affect the haematopoietic system, but it exhibits neuroprotective and neurotrophic properties in the central nervous system and in the retina. Both the erythropoietin and its receptor (EPOR) are expressed in the retina, however, their cellular distribution and physiological role are not known. In the present study, we examined developing postnatal and adult rat retinas by EPO- and EPOR-specific antibodies with single and double labeling techniques in order to identify the temporal and spatial onset of their expression in the mammalian retina.

Retinas from Sprague-Dawley rats of different developmental ages were collected and analysed by immunohistochemistry. Following fixation and cryoprotection 10 µm thick frozen sections were cut from each specimen and stained with EPO and EPOR-specific antibodies. In double labelling experiments the horizontal cell-specific anti-calbindin antibody and the cone-specific marker PNA were also used. The labelling was visualised by the ABC method or by fluorescent antibodies and analysed by light or confocal microscopy.

At the time of birth the EPO-specific staining resulted a strong cytoplasmatic labelling in the ganglion cell layer and a weak, diffuse staining in the neuroblast layer. On the following days strong membrane immunoreactivity appeared in the developing horizontal and amacrine cells, and by the end of the first postnatal week the entire inner nuclear layer became positively stained. From the beginning of the second postnatal week on immunopositivity in the inner and outer plexiform layers and in the developing photoreceptor processes was also observed. The same result was found in the adult, where the cells of the ganglion cell layer and the inner nuclear layer, both plexiform layers and the photoreceptor inner segments bound the EPO-specific antibody. The staining pattern of the EPOR-specific antibody and the time of onset of the immunopositive elements showed big similarity to that of the EPO-specific antibody.

Since the spatial and temporal onset of the expression of the erythropoietin and its receptor correlates with the postnatal developmental events of rat retina, our findings suggest the involvement of the erythropoietin in the regulation of cell maturation, developmental apoptosis and synaptogenesis.

OTKA#T-042524, OTKA#F-61717.

*Corresponding author
E-mail: vegvari_dora@freemail.hu

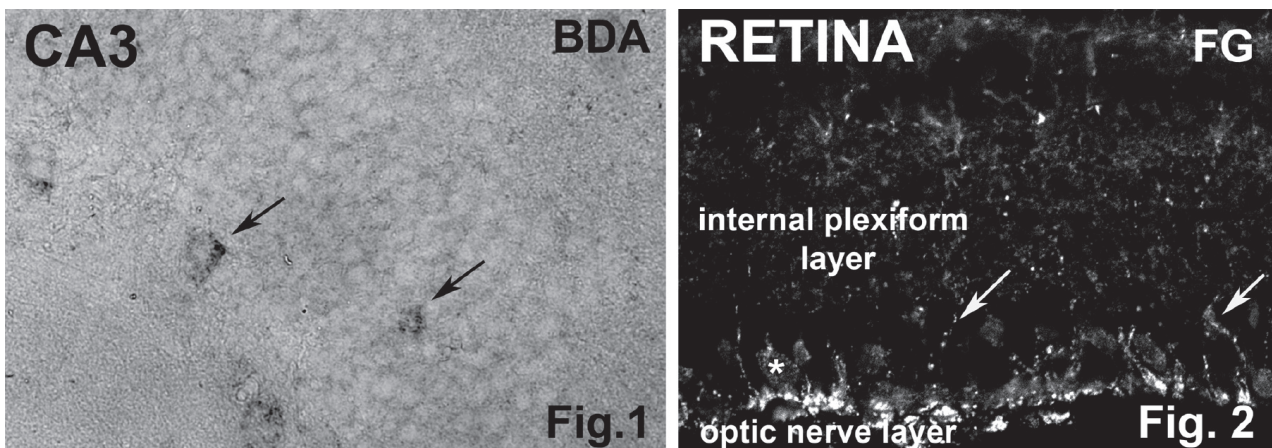
Centrifugal visual fibers arising from the limbic system and the hypothalamus

V Vereczki^{1*}, Á Csáki², GE Hoffman³, G Fiskum⁴, K Kovcs²

¹Department of Anatomy, Histology and Embryology, Semmelweis University of Medicine, Budapest, Hungary, ²Department of Human Morphology and Developmental Biology, Semmelweis University of Medicine, Budapest, Hungary, ³Department of Anatomy and Neurobiology, The University of Maryland School of Medicine, Baltimore, MD, USA, ⁴Department of Anesthesiology, The University of Maryland School of Medicine, Baltimore, MD, USA

It is already known that the optic nerve contains centrifugal fibers which are positive to VIP, LHRH or PACAP, but their origin had not yet been fully elucidated.

In our experiments utilizing the retrograde and anterograde transport of tracers (biotinylated dextran amine[BDA] and Fluorogold [FG], respectively) we have provided direct evidence for the cells of origin of a limboretinal and hypothalamoretinal pathways in rats and the termination of the centrifugal visual fibers in the retina using light microscopic approach. With the use of adult male rats following intravitreal injection of 10 000 kD BDA into the right eye, we have found retrogradely labeled



BDA neurons in subregions of the hippocampus (in CA1, CA3) and dentate gyrus at both sides. We have also observed BDA containing neurons in the induseum griseum, lateral habenulae and in the olfactory tubercle. In the hypothalamus 1-2 BDA positive cells were seen in the lateral accessory magnocellular and in the supraoptic (SO) nuclei. The major part of labeled cells were observed in the hippocampal formation (Fig. 1, arrows indicate labeled cells). It was estimated that the total number of retrogradely labeled cells in this formation is 1495 ± 516 . We have seen fiber labeling in the retinorecipient suprachiasmatic nucleus and in the primary visual center, the lateral geniculate body, but labeled nerve cell bodies in these structures were never seen indicating that the tracer was transported anterogradely in these structures. Iontophoretic administration of FG into the hippocampal formation, where the major part of BDA labeled cell bodies were observed, has resulted in labeled fibers in the optic nerve and in the retina at both ipsi- and contralateral sides indicating that the retrogradely labeled cells in the hippocampus and the dentate gyrus among others are the cells of origin of centrifugal visual fibers (Fig. 2, arrows indicate FG labeled fibers in the internal plexiform layer, * shows an unlabeled ganglion cell). Double labeling revealed that the retrogradely labeled neurons in the hippocampus were also positive to LHRH or to VIP or to PACAP. Some of the BDA positive cells in the induseum griseum and in the olfactory tubercle were LHRH immunopositive, and some of them in the SO and in the dentate gyrus were PACAP immunopositive, and some of them in the dentate gyrus were VIP immunopositive. On the basis of our results it was concluded that the abovementioned structures of the limbic system and the hypothalamus send LHRH, VIP and PACAP containing fibers to the retina where they terminate. The potential importance of these centrifugal fibers remain unknown, but like in other sensory organs, they provide central feedback to this sensory system and they might influence the visual input of the retina to the central nervous system.

*Corresponding author
E-mail: koves@ana2.sote.hu

Cerebrospinal fluid-contacting neurons, the role of their various receptors and axon terminals in the nonsynaptic signal transmission

B Víg^{1*}, Cs Dávid¹, Zs Fejér¹, A Magyar¹, L Szabó², Á Szél¹

¹Department of Human Morphology and Developmental Biology, Semmelweis University, Budapest, Hungary, ²Department of Pathology, Albert Schweitzer Hospital, Hatvan, Hungary

The system of cerebrospinal fluid (CSF)-contacting neurons represent special nerve cells taking up, transforming and emitting nonsynaptic signals mediated by the CSF. Most of them send dendritic processes bearing sensory cilia into the brain ventricles and central canal and are similar to known sensory cells of chemo-, mechano- and/or photoreceptor-type (Fig. 1). The axons of the CSF-contacting neurons transmit information taken up by their dendrites to synaptic zones of various brain areas or form neurohormonal terminals releasing various bioactive substances to the external CSF space. Some of their axons enter the internal CSF, terminating there by free endings. Sensory-type cilia were also found to extend into the intercellular spaces from nerve cells situated in various brain areas including brain cortex.

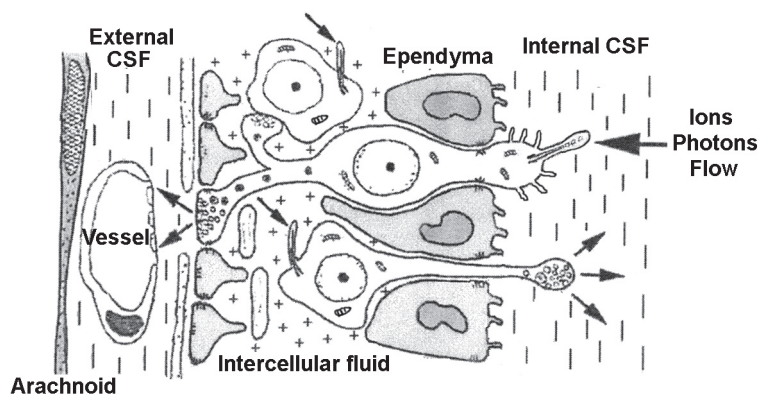


Figure 1. CSF-contacting neurons. Arrows: neurohormonal and nonsynaptic signaltransduction.

Some secondary neurons of the retina and pineal organ directly contact the retinal photoreceptor space (Landolt' clubs) and pineal recess, respectively. The composition of the fluid of the photoreceptor space and the CSF of the pineal recess may modify the activity of these neurons. CSF-contacting neurons representing the deep encephalic photoreceptors contain various opsins and detect the illumination of the brain tissue and play a role in the circadian periodicity of the organ.

CSF-contacting dendrites of the oblongate medulla, spinal cord and terminal filum bear kinocilia, and resemble mechano-receptors. Terminating at the external CSF-space, the axons of these neurons form neurohormonal nerve endings.

This work was supported by the Hungarian OTKA grant No. T 29048.

Vigh B, Fejér C, Dávid C, Szél A (2007) Neurosecretory axon terminals: special nerve endings for release of bioactive molecules. Nova Science Publishers, Neural Synapse Research Trends Chapter VI. pp. 1-24.

Vigh B, Manzano e Silva M J, Zádori A, Frank C L, Lukáts Á, Röhlich P, Szél A, Dávid C (2002) Nonvisual photoreceptors of the deep brain, pineal organs and retina. *Histol Histopathol* 17:555-590.

*Corresponding author
E-mail: vigh@ana2.sote.hu

Migration of mouse sacral neural crest cells from the neural tube to the hindgut

X Wang¹, AK Chan¹, SY Cheung¹, TF Wan¹, AJ Burns², WY Chan^{1*}

¹Department of Anatomy, Faculty of Medicine, The Chinese University of Hong Kong, Hong Kong, ²University College London, Institute of Child Health, UK

Neural crest cells are a group of migratory embryonic cells which emerge from the neural tube and migrate along defined pathways to various locations throughout the embryo. Studies in avians have shown that sacral neural crest cells initially form an extramural nerve, the nerve of Remak, then migrate into the caudal hindgut and contribute a significant number of neurons and glial cells to the hindgut enteric nervous system. A similar population of sacral neural crest cells has been shown to form the extramural pelvic plexus in mammals but information on the migration of mammalian sacral neural crest cells to and within the hindgut is still scarce. To trace the migration of sacral neural crest cells from the neural tube to the mouse hindgut, we first used *in situ* labelling of pre-migratory sacral neural crest cells with wheat germ agglutinin-gold conjugates (WGA-Au) followed by whole embryo culture to determine the initial migration from E9.5 to E10.5. We then mapped immunohistochemically neural crest cell migration from E11.5 onwards with an antibody to the neurotrophin receptor p75^{NTR}, which is expressed in all neural crest-derived cells in the gut. The spatio-temporal distribution of labelled cells was analyzed with confocal microscopy and 3-dimensional images of the embryos were reconstructed from serial sections. Sacral neural crest cells caudal to somite 24 were found to start their migration in embryos with 27-28 somites and they traversed dorsomedially through the mesenchyme between the somites and the neural tube to reach the peri-aortic region within 24 hours. Some of these cells continued to migrate more ventrally and exhibited p75^{NTR} immunoreactivity. The pioneer neural crest cells (the most ventrally located p75^{NTR+} cells) were found in regions dorsolateral to the caudal hindgut at E11.5 and on the lateral sides of the hindgut at E12.5. By E13.5, neural crest cells (p75^{NTR+}) were found in pelvic plexi ventrolateral to the caudal hindgut but no p75^{NTR+} cells were found in the caudal hindgut. However, at this stage, vagal neural crest-derived enteric cells (also p75^{NTR+}) had already advanced to colonise the rostral half of the hindgut. At E14.0, when the rostral two-thirds of the hindgut had been colonized by vagal neural crest-derived cells, isolated p75^{NTR+} cells were apparent in the terminal hindgut. At this stage a hindgut region of about 800 µm remained devoid of any positive cells. This uncolonised region was located between the rostral (vagal neural crest-derived) and the caudal (probably sacral neural crest-derived) groups of p75^{NTR+} cells. Streams of p75^{NTR+} cells were also found on the ventral side of the hindgut connecting the pelvic plexi with the terminal hindgut at the sacral level of S2/S3. At E14.5, the entire length of the hindgut was fully colonized by p75^{NTR+} cells. We therefore conclude that sacral neural crest cells begin to enter the terminal hindgut via pelvic plexi at E14.0 at the sacral level of S2/S3, prior to the arrival of vagal neural crest cells in the caudal hindgut.

The work described here was supported by a grant from the Research Grants Council of the Hong Kong Special Administrative Region, China (Project No. CUHK4418/03M).

*Corresponding author
E-mail: wy-chan@cuhk.edu.hk

The concentration-dependent neo- and allocortical effect of GYKI 52466 in the 4-aminopyridine-induced acute rat seizure model

R Weiczner*, B Krisztin-Péva, A Mihály

Department of Anatomy, Histology and Embryology, Faculty of Medicine, University of Szeged, Szeged, Hungary

The activation of ionotropic glutamate receptors leads to the expression of transcription factor *c-fos* via protein-phosphorylation cascades. In former studies we have proved that the antagonists of N-methyl-D-aspartate (NMDA)-receptor significantly reduce the *c-fos* gene expression in 4-aminopyridine (4-AP)-induced acute convulsions in the rat cerebral cortex. In the present study we have examined the supposed relation between the activation of α -amino-3-hydroxy-5-methyl-4-izoxazol-propionate (AMPA)-receptors and *c-fos* expression in 4-AP-induced convulsions. According to our previous data, the seizure activity is accompanied by oedematous changes in the astrocytic endfeet around the cerebral capillaries.

As an antagonist of the AMPA-receptor, GYKI 52466 has been administered in 25 and 50 mg pro bwkg doses, intraperitoneally. The control groups received the solvent of this antagonist. Then, acute convulsion was elicited by the intraperitoneal administration of 4-AP (in 5 mg/kg dose) in pretreated and control groups, as well. The latency of the well-defined seizure symptoms was measured. After one hour observation time, the animals were sacrificed, the brains processed either for double-labelling light microscopic immunohistochemistry, (for *c-fos* and parvalbumin (PV) detection) or for electronmicroscopy (capillary lumen area and surrounding oedematous changes); focusing on the parietal neocortex and on the hippocampus. The number of immunoreactive cell nuclei pro area unit (mm²) was quantified and the capillary and pericapillary areas were measured, then statistical analysis was performed on the gained data.

In the AMPA-antagonist pretreated groups the latency of generalised tonic-clonic seizure (GTCS) was prolonged, no recurrent seizure was observed; the survival of the animals was 100%. In the neocortex, the higher antagonist dose caused a significant decrease in *c-fos* expression, mainly in the neocortical II-III and V-VI laminae. This effect was present in case of *c-fos* + PV double-labelled cells in a dose-dependent fashion. In the examined allocortical areas even the lower dose antagonist pretreatment moderated significantly the *c-fos* positive and *c-fos*+ PV double-labelled cell count. The lower dose pretreatment seems to be aggravate the oedematous changes, whereas the effect of the higher dose pretreatment statistically is not contributive. The reduction of this activity-dependent neuronal marker was more remarkable in the allocortical than in the neocortical areas, pointing to the difference in the AMPA-receptor distribution. To decrease the *c-fos* expression in PV-positive cells, a lower antagonist dose was sufficient enough, showing the significance of the AMPAergic input of this cell subpopulation. According to the statistical data, the AMPAergic mediation may not be the primary component influencing the oedematous changes of the pericapillary areas in the rat brain.

Szakács R, Weiczner R, Mihály A, Krisztin-Péva B, Zádor Zs, Zádor E (2003) Non-competitive NMDA receptor antagonists moderate seizure-induced *c-fos* expression in the rat cerebral cortex. *Brain Res Bull* 59:485-493.

Mihály A, Szakács R, Bohata Cs, Dobó E, Krisztin-Péva B (2001) Time-dependent distribution and neuronal localization of *c-fos* protein in the rat hippocampus following 4-aminopyridine seizures. *Epilepsy Res* 44:97-108.

Fabene PF, Weiczner R, Marzola P, Nicolato E, Calderan EL, Andrioli A, Farkas E, Süle Z, Mihály A, Sbarbati A (2006) Structural and functional MRI following 4-aminopyridine-induced seizures: a comparative imaging and anatomical study *Neurobiol Dis* 21:80-89.

*Corresponding author

E-mail: weiczner@anatomy.szote.u-szeged.hu

Garlic extracts working in concert with docetaxel to suppress the growth of androgen independent (AI) prostate cancer

YC Wong*, E Howard, XH Wang

Cancer Biology Lab, Department of Anatomy, Li Ka Shing Faculty of Medicine, The University of Hong Kong, Pokfulam, Hong Kong, HKSAR, China

Androgen independent prostate cancer (AIPC) is an end stage prostate cancer characterized by bone metastasis and with few therapeutic options. Docetaxel has been shown recently to have significant effect on treatment of AIPC but unfortunately the strategy, though significant statistically, was modest with only about 2.5 months in survival advantage due to intolerance and resistance to docetaxel therapy. Recently we have shown that garlic extracts such as SAC (S-allylcysteine) and SAMC (S-allylmercaptocysteine) could effectively suppress the proliferation, migration and invasion of AIPC cells under in vitro condition (Chu et al. 2006). This inhibitory effect was associated with induction of mesenchymal to epithelial transition. More importantly, the SAC and SAMC treatment led to restoration of E-cadherin expression while the expression of E-cadherin repressor, Snail, was downregulated. We have also studied the effect of these compounds on prostate cancer under in vivo condition using CWR22R, an AI prostate cancer xenograft in nude mice. The results showed that treatment with the garlic derivatives inhibited the growth of CWR22R without any detectable toxic effect on nude mice. The SAC and SAMC induced growth reduction was correlated with a reduction in serum PSA level and proliferation rate of xenografts (Chu et al. 2006). Our latest study revealed that SAMC could sensitize the action of docetaxel on AIPC under both in vitro and in vivo conditions. Overall our results suggest that these garlic derivatives may be potential therapeutic agents for the suppression of AI prostate cancer either alone or as a potent adjunct to docetaxel therapy for AIPC patients. Combination of garlic extract with docetaxel may allow lowering of the latter dosage, thus enhancing the effectiveness of docetaxel on one hand while reducing the toxicity on the other hand. [Supported by AICR (05A006-REV2) and RGC grants (HKU7478/03M) to XHW and YCW (HKU7490.03M, 7470/04M, NSFC/RGCN HKU738/03, HKU Foundation Seed Fund, 03)].

Chu QJ, Ling MT, Cheung HW, Wang G, Tsao SW, Wang XH, Wong YC (2006) A novel anticancer effect of garlic derivatives: inhibition of cancer cell invasion through restoration of E-cadherin expression. *Carcinogenesis* 27:2180-2189.

Chu QJ, Lee DTW, Tsao SW, Wang XH, Wong YC (2006) S-allylcysteine, a water soluble garlic derivative, suppresses the growth of CWR22R, a human androgen-independent prostate cancer under in vivo condition. *British J Urology International* 99:925-932.

*Corresponding author

E-mail: ycwong@hkucc.hku.hk

Analysis and standardization of the anastomoses between the segmental branches of the portal hepatic vein. Study on corrosion casts

DE Zahoi, P Matusz*, AM Pusztai, D Sztika, E Pop

Department of Anatomy, Faculty of Medicine, University of Medicine and Pharmacy Victor Babes Timisoara, Romania

The right and left branch of the portal hepatic vein are placed into the fissures of the venous segmentation of the hepatic parenchyma, areas considered as paucivascular from the point of view of the elements forming the efferent pedicle of the liver (hepatic veins and their affluents). The right branch of the portal hepatic vein gives birth to the anterior and to the posterior branch. From the umbilical portion of the left branch arise the medial branches and the lateral branches. The lateral branches (superior and inferior) go to the left lateral division (S II and S III), the medial branches go to the left medial division (S IV), the anterior branch goes to the right medial division (S V and S VIII) and the posterior branch goes to the right lateral division (S VI and S VII). Numerous authors described liver's parenchyma segmentation based on the terminal character of the branches of the portal hepatic vein. All the same, in the anatomical literature anastomoses between the segmental branches of the portal hepatic vein are described in the normal liver. In order to demonstrate the anastomoses between the segmental

branches of the portal hepatic vein in the normal liver, we analyzed 100 hepatic corrosion casts (from persons without previous liver disease). The livers were injected with plastic (AGO II paste and TECHNOVIT 7143), followed by hepatic parenchyma corrosion with hydrochloric acid. We found 16% cases with anastomoses between the branches of the portal hepatic vein. In 12% cases the anastomoses were intersegmentary (mostly unique anastomosis in 91.67% cases, 11/12 casts, and in one case out of 12 two intersegmentary anastomoses – 8.33% cases). In 4% cases we found anastomoses between portal branches of the same segment (intra-segmentary anastomoses). In case of portal intersegmentary anastomoses, in 50% cases (6/12 casts) was involved a portal branch belonging to segment IV. The portal intersegmentary anastomoses most often intersected the plane of the right portal fissure (58.33% cases, 7/12 casts). In case of the 4 portal intra-segmentary anastomoses, 50% (2/4 casts) were located in the parenchyma of the segment VIII (one between two branches of III-rd order and the other between a branch of the III-rd order and the posterior branch of the hepatic portal vein). The overall analysis of the intraparenchymal distribution of the anastomoses of the branches of the hepatic portal vein showed 11 morphological types of distribution in the case of portal intersegmentary anastomoses. The analysis of the position of the portal anastomoses at the level of each portal fissure shows the following: at the level of the umbilical fissure, both the anastomoses between the segmental branches S II – S IV and S III – S IV are situated anterior to the trunk of the left hepatic vein; at the level of the main portal fissure the anastomoses between the segmental branches S IV – S V and S IV – S VIII are situated next to the anterior aspect of the trunk of the middle hepatic vein; at the level of the right portal fissure the portal anastomoses between S V – S VII and S VII – S VIII are situated in a plane superficial to the trajectory of the right hepatic vein (single or multiple). Knowing these aspects of morphologic interrelation between the branches of the hepatic portal vein at intersegmentary level could facilitate the planning of surgery for liver resection or transplant.

Supported by CEEEX 175/2006.

*Corresponding author
E-mail: matusz@umft.ro